

Response to referee comments regarding Herreid and Pellicciotti, “Automated detection of ice cliffs within supraglacial debris cover”

<https://doi.org/10.5194/tc-2017-151>

February 14, 2018

Comments from David Rounce (RC1)

We would like to thank David Rounce for his careful, detailed and very helpful comments. His point regarding the 3D consideration of the entire spatial domain was improved the quality of our results. We first address his general comments and then respond, point by point, to his specific comments. Reviewer comments are indented with a grey bar with our response below.

This study develops a new method to map ice cliffs based on the slope of a highresolution (< 5 m) DEM. The method is developed on Canwell Glacier in Alaska and compared to ice cliffs that were delineated from high resolution visible and thermal images. The method was also applied to Ngozumpa Glacier, where a pre-existing dataset of ice cliff delineations used to assess the method’s broader applicability. The developed method is quite novel in its use of a centerline extension length, which enables the method to capture the smaller ends of the ice cliffs. Another novel part of the method is the generation of probability maps and the assessment of the model’s performance, which enables the accuracy and precision to be properly assessed. For the most part, the manuscript is very well written and easy to follow. The problems associated with mapping ice cliffs are well described as is the relevance of this study. Specifically, ice cliffs on debris-covered glaciers are localized areas of high melt such that they can significantly alter the evolution of debris-covered glaciers; however, mapping ice cliffs remains difficult. The methods developed in this study are a major advance and will be a significant improvement once high resolution DEMs are available on a global scale. The only general comments I had were concerning the use of 2D area versus 3D area and the accuracy of the validation datasets. All other comments were very minor. All in all, I believe this study is a sound contribution to the field and recommend this study for publication after minor revisions.

One of the major improvements of this method is the ability to estimate the 3D area of the ice cliffs as opposed to 2D area typically derived from nadir-looking satellite imagery. First off, the authors refer to these areas in a variety of different ways throughout the text, e.g., true ice cliff area, area considering slope, and 3D area. While they are fairly easy to understand, it may be clearer for the reader to use one set of terminology throughout the paper.

We agree that several terms are used to describe the same quantity (true ice cliff surface area, area considering slope, 3D surface) but we think that depending on the context each makes sense, e.g. if discussing a comparison to map-view surface area, it is the most intuitive to use ‘true surface area’ while when discussing the various methods for ice cliff mapping, it seems best to talk in 3D, 2D, 1D terms. At the first mention of a 3D surface (Section 3.2.1) we have added “...are converted to 3D surfaces (...used synonymously with ‘true surface area’ and ‘area considering slope’).” and at many location where we say ‘true surface area’ we in parenthesis say “area considering slope”. If the Reviewer or Editor disagree and find this to be unnecessary confusion we are happy to select one and be consistent throughout.

Furthermore, when comparing 2D area and 3D area (Section 4.1), the authors state the ice cliffs make up 4.9% of the map view area, but that this underrepresents the true area by 19%. This seems to imply that the true ice cliff area would be 19% greater (6%) of the total glacier area; however, that does not factor into account what the true glacier area would be. I wonder how much the ice cliff area changes compared to the 3D glacier area? If this is substantial, then it would highlight the importance of assessing 3D area, while if it is negligible it may indicate that using 2D area is sufficient. Either way it could have important implications for modeling the evolution of debriscovered with ice cliffs included.

This is a very useful comment, and the reviewer is right that there are differences between the 2D and 3D areas, which we have neglected to consider. We have now calculated the 3D area and updated Section 4.1 to included 3D glacier area. There is a difference of the percentage of ice cliffs within the study area from 4.9% in map view to 5.7% considering slope.

I found the discussion of how an ice cliff is defined to be very interesting. Specifically, determining how thin debris that is typically present on ice cliffs is considered is a challenging problem. The high resolution thermal imagery truly enabled this problem to be investigated, but I wonder how the authors ‘‘liberal outlines’’ influenced the ice cliff area? Is there a way to estimate the percentage of ice cliffs that were easy to include versus those that were questionable? Were the additional ice cliffs that were added to Ngozumpa Glacier all these questionable ice cliffs? If so, the percentage that was added could provide some indication as to the difference in ice cliff area that different individuals may have. Furthermore, this may enable the authors to quantify the uncertainty associated with the validation dataset, which did not appear to be considered, i.e., this is different than the uncertainty associated with the developed method compared to the validation dataset.

There are several good points and questions within this comment. Subjectivity is an often under quantified variable in manually generated data. A common approach to quantifying subjectivity is having several technicians conduct the same mapping task independently and compare the variability between technicians. While this is a worthwhile method, it is still limited to the data the technicians are given and their personal mapping criteria which could both contribute to a converging result that is still not ‘true’. For this study we tried a different approach to minimizing subjectivity by collecting corroborating datasets. By using high resolution visible and thermal data we were able to cross validate our ice cliff outlines. However, even with these data we found the manual mapping difficult as there was a continuous spectrum of ice cliffs between easily identified to questionable identification. Because of this spectrum we don’t know of a robust way to delimit ice cliffs between easy and questionable identification. To make this distinction clear we added to Section 3.4: “While we made an effort to manually map ice cliffs based on consistent criteria, there is subjective interpretation within this ‘truth’ dataset. We did not quantify the uncertainty associated with this subjectivity.” Regarding Ngozumpa Glacier, our preference would have been to make no additions to the ice cliff map, yet we also thought that the mapping criteria should be consistent with how we mapped ice cliffs for Canwell Glacier. Of the ice cliff additions we made, 9 had what we would call a considerable “thin” debris covering, 7 were in dark shadow making a very confident classification difficult, 4 were what we would interpret as omission errors and several of these and around 13 others were quite small. Because of the variable reasons for omission, it is not clear to us what can be considered questionable. If two technicians independently zoom in to a region and agree there is a small ice cliff but for further mapping one technician maps from only half the zoom and no longer finds small ice cliffs while the other does, are the missed small ice cliffs questionable or not questionable? We very much like the the questions raised but did not attempt to quantify the inherent subjectivity.

Specific comments

P1, L5: ‘‘include’’ not included.

Correction made.

P1, L14-16: Sentence is difficult to read. Perhaps, ‘... are still poorly understood processes, in part, due to a lack of base data, which is an obstacle for establishing a robust understanding...’

Changed as suggested with an additional shortening of the sentence.

P1, L20-21: present on a debris covered glacier

Changed as suggested.

P2, L16-17: ‘a small area of low angle... enclave’ does not make sense. Both area and enclave are referring to a specific area, so it is difficult to understand.

Changed to “...a small area of low angle (i.e. not cliff) bare glacier ice located within a debris-covered portion of a glacier...”

P3, L2-3: ‘North and south facing ice cliffs will likely be optically distinct and crescent to circular ice cliffs will exhibit’ does not make sense. Please clarify what you are trying to say.

Changed to: “North and south facing ice cliffs present in a single image will likely appear either dark (shaded bare ice) or light (illuminated bare ice) relative to unshaded surrounding debris cover. Crescent to circular ice cliffs will likely exhibit a spectrum of shade and illumination.”

P3, L28: ‘identify’ not identifying

This sentence has been removed in response to a comment below.

P5, L26-32: ‘Ngozumpa Glacier was selected for two reasons, first, ...’. The second reason does not appear until Line 32 making it difficult to following what the two reasons are. I would suggest either making it two separate sentences and keeping it the same, i.e., \Ngozumpa Glacier was selected for two reasons. First, ...” or state the two reasons in that sentence and then go on to describe them

Changed as suggested: “Ngozumpa Glacier was selected to be used in this study for two reasons. First, it is”.

P5, L26-27: this sentence is repetitive. Distinctly different geographical location and notably different from Canwell Glacier mean the same thing.

We agree the initial wording was repetitive. We have added more details to clarify our point: “First, it is located in a geographical region that is different from the Alaska Range with respect

to latitude, longitude, continentality, climate and orogeny. These factors and others establish a setting where exposure to the sun and the overall debris cover (e.g. debris extent, clast sizes, and thickness) at Ngozumpa Glacier is notably different from the Canwell Glacier.”

P7, Eqn 1: Why the use of Y and N as opposed to 0 and 1, which is more typical of a binary system?

Changed as suggested.

P7, L23: “Where” does not need to be capitalized. Also, does the paragraph after an equation, which is still part of the previous paragraph need to be indented? If not, then change this after all equations.

With particular respect to P7 L23 we ended the sentence with Eq. 1 to avoid a very run on sentence, but are happy to change this at the Editor’s request. We corrected the indentations here (P7 L23) and throughout as suggested.

P8, L8: Is the $A_{cliff,i}/area(\text{spatial domain})$ a comparison of 3D cliff area to 2D glacier area? If so, this seems as though you are comparing apples to oranges and it should be 3D area to 3D area or 2D area to 2D area.

The quantity $A_{cliff,i}/area(\text{spatial domain})$ described at P8, L8 is a ratio of two 2D areas. To help eliminate confusion we have added the sentence at the beginning of Section 3.2.1: “This area, and all subsequent areas derived in the mapping method, are simplified as a shape in two dimensions (2D). Only final results of the mapping method are converted to 3D surfaces (Sect. 4 and 5.3, method described in Sect. 3.4).”

P9, L16-17: I would recommend changing this to the positive instead of using a double negative { ‘‘it is critical that segments are large enough such that meaningful statistics can be computed’’}.

Changed as suggested.

P10, L15: Once again, ice cliff area is 3D, but is the glacier 3D area also considered in this manner? I would imagine this would impact the area associated with false positives, etc.

For the statistical measures of performance analysis we consider only 2D area. 3D true surface area is only used when presenting final (more science question oriented) results. The majority of the article is focused on mapping and a consistent use of 2D surface area simplifies the problem. We have made this more explicit in P10 L15: “True surface area (as opposed to map view surface area) was calculated to present final results (Sect. 4 and 5.3) by multiplying...”

P11, L28: Is thin debris cover quite sensitive to this pixel value threshold? Does it greatly alter the percentage of thin debris on the ice cliffs?

We did not conduct a quantitative sensitivity analysis and have added this caveat to the text: “We did not quantify the sensitivity of this threshold parameter and relied on visual assessment (e.g. comparing panels b and c to panels d and e in Fig. 7) to determine a single values that minimized errors (e.g. due to varying lithology)and maximize success.”

P12, L6-7: How does the 19% increase alter the percentage of the total glacier area (3D in this case)? See the General Comment

The text has been updated with the following new information: “The manually generated, ‘true’ ice cliff dataset shows 4.9% of the 1.74 km² Canwell Glacier study area is ice cliff in map view (not considering slope). Ice cliff map view area (84,630 m²) under represents true ice cliff surface area (104,920 m², considering slope) by 19%. Considering the true surface area of the Canwell Glacier study area, map view under represents true surface area (1.86 km²) by 6%. Considering both true surface area of ice cliffs and the Canwell Glacier study area, the fraction of ice cliff area is 5.7%.”

P13, L16: I would suggest stating the distance from the terminus of the lower ablation zone or state the area that was investigated based in Section 2.2.2. It’s shown in Figure 1, but it may be nice to have the text as well.

Changed as suggested.

P13, L24-25: Sentence is confusing. Please clarify. Specifically, what is assumed to be transferable to Ngozumpa Glacier? The model input parameters, the methods?

Changed to: “Considering that not a single alteration was made to the method and input parameter values used for Canwell Glacier, the method mitigated the many physical differences between Canwell and Ngozumpa glaciers (described in Sect. 2.2.2 and shown in Fig. 3) as well as different DEM generation methods (satellite based rather than airborne structure from motion). This ability to accommodate different physical characteristics enables the method to outperform a simple slope threshold found at one location, e.g. at Canwell Glacier, and assume that it is transferable to other places on Earth, e.g. Ngozumpa Glacier (Tables 2 and 3)”

P14, L6: \tested" not testing

Correction made.

Section 5.3: The use of high-resolution thermal imagery to map ice cliffs seems to be invaluable in assessing the thin debris on ice cliffs. I am surprised that this important dataset is not mentioned with respect to future work, i.e., while higher resolution DEMs will enable this method to be applied, it appears that high resolution thermal imagery is needed to assess the accuracy of the methods in other areas, correct?

We believe this is correct but were also hesitant to be too explicit when making suggestions to future scientists, perhaps there is even better validation data that we have not thought of. We altered a sentence in Section 6 to: “Further validation of this method using ice cliff maps from high resolution visible, thermal or other data in other regions will help to either support or discredit our claim of wide applicability.”

Table 2. Appear to be missing blue/best error distribution?

Correction made.

Table 3. No bold font as alluded to in the caption. Also, no red TP rate or blue error distribution?

Correction made, with additional cells added to clarify now more precise corresponding text in Section 4.2.

Figure 1. For someone not familiar with Ngozumpa and Canwell Glaciers it may be difficult to determine which glacier is which. I would recommend stating left and right or placing (a), (b), and (c) on the figures.

Changed as suggested with left and right in the caption.

Figure 3. There are 3 colors in the inset plots and yet only 2 colors in the legend. What is the third color representing?

Changed as suggested.

Sentence added to the caption of Figure 3: “The grey/orange region of overlap illustrates the difficulty of using surface slope alone to identify ice cliffs.”

Changed as suggested.

Figure 4. May be nice to show Le on both sides

We think it is sufficiently clear with one label given the color difference and the legend directly above, but are happy to add this at the Editor’s request.

Figure 5. The surface temperatures are counter-intuitive. Red is cold and blue is hot. Figure 10 has them as red is hot and blue is cold. I would recommend switching these such that they are intuitive and consistent.

This was an intentional deviation from consistency and intuition, now explained in the caption: “The color gradient is flipped so that cold ice cliffs easily stand out as red can be easily compared with [panel] (d).”. We can still change this if the reviewer/editor is not convinced by our argument.

Comments from Anonymous (RC2)

We thank Reviewer 2 for her/his careful, detailed and helpful comments. We were especially appreciative of the close attention to mathematical details. We first address her/his general comments and then respond, point by point, to her/his specific comments.

This manuscript tries to facilitate a more robust and operator-independent mapping of ice cliff extent on debris covered glaciers. The method is based on an investigation and classification of local surface slopes, using raster elevation maps (e.g. satellite derived DEMs). In order to assess the usefulness of such an approach, it might be worthwhile to discuss the reasons, why ice cliffs should be mapped at all. Ice cliffs are steep, smooth sections of glacier surface with no, or only a minor coverage of supra-glacial debris, embedded in glacier area with a considerably thicker debris cover. Due to this difference in debris thickness and the fact that the thin debris cover on the ice cliffs usually is below the critical thickness of the Östrem curve, these areas tend to show a strongly enhanced melt rate compared to the surrounding glacier surface. Also, the aspect and slope of ice cliffs can be favorable for melt. The crucial parameter, which relates potential ice melt to atmospheric parameters, in this context, is the surface temperature. In fact, it is not really necessary to call something an ice cliff, if high melt rates can be derived or parameterized from other information. Unfortunately, the map view area of ice cliffs is usually much less than the available pixel resolution of thermal remote sensing products. The availability of higher resolution DEM information might therefore be a good reason to try and identify such areas of high ice loss from geometric constraints.

We completely agree that there may be other approaches or datasets that could make the mapping of ice cliffs (especially through geometric constraints) obsolete. However, as the reviewer points out, at the present time more favorable datasets have not yet become available or have not yet been exploited/introduced into the debris covered glacier research community. While something more robust will surely emerge it is with the goal of addressing large scale problems now that motivated the writing of this paper. We added to the second sentence of the introduction a stated link between resolving where ice cliffs are with respect to solving for glacier melt in heavily debris-covered regions.

This manuscript demonstrates a novel approach to investigate the slope distribution across debris covered glacier surfaces and relates these results to the probability of ice cliff existence. In my view, this is a considerably advance towards automated ice cliff mapping, based on the availability of remote sensing products. Even though the authors discuss the problems connected with ice cliff definition, the main problem I see is the missing link between the classification tool and the physical conditions for ice cliff generation. The basis of the method is a threshold for surface slope, above which a slope can be considered an ice cliff. Furthermore, the probability of ice cliff occurrence is computed for a series of thresholds, producing a Gaussian distribution function of ice cliff fraction versus slope threshold. The optimum choice of slope threshold is then found as the intersection of the maximum orthogonal distance between a hypothetical line P1-P2 and the distribution function. I cannot see any physical reason why this should be a ‘‘preferred’’ angle in the distribution function. On page 8, line 22 it is clearly stated that this is hypothesized, but there is no attempt further in the manuscript relate that to any physical characteristic. Maybe I missed the point, but I would encourage the authors to improve this relation between the distribution function and the conditions defined as requirement for ice cliff existence. In this context, it might also be worth to discuss the choice of a Gaussian distribution function, which relates to the reasons for surface undulations on the glacier surface. Basically, it can be assumed that strain, differential melt and the existence of surface melt water are responsible for the creation of surface undulations. If these effects are randomly distributed, a Gaussian distribution function is probably a good representation. This, however, can be questioned with regards to ice cliffs, because these features are usually connected with a discontinuity in surface slope. The reason for this is that the ice cliff surfaces are not able to maintain the original debris cover and melt rates change abruptly at the cliff boundaries, leading to characteristic cliff slope angles. Besides this lacking linkage between the statistical model and the physical world, this manuscript is a valuable contribution to the important issue of including ice cliffs in the mass balance estimates of debris covered glaciers

Firstly, we made a semantic error that misled the reviewer. While the shape of Eq. 2 is that of a Gaussian distribution, we were not using it to model a distribution, we were simply fitting a model to data and the shape of Eq. 2 fit the data well. Since the single objective of this study was mapping existing ice cliffs, a discussion of physical conditions for ice cliff generation is out of the scope of this work, and reflects the fact that, despite major recent progresses in our understanding of ice cliffs over debris covered glaciers, we still know too little about cliff generation in particular. We do thank the reviewer for pushing us to consider the physical reality that underpins hypothetical lines and ‘‘preferred’’ angles. At P.8 L.22 [location in original submission] we tried to fully describe the hypothesized relation of an optimum slope threshold with physical characteristics: ‘‘The hypothesis is that as β_i increases and less sloped debris-covered area (e.g. from strain and differential melt) is included as mapped ice cliff, true ice cliffs will begin to comprise the majority of the mapped ice cliff fraction (y_i). We hypothesize

this to have a stabilizing effect (ice cliffs are a small, consistently steep area), lowering the rate of loss of mapped ice cliff area and slope of the curve as β_i continues towards 90° . We hypothesize that this so-called ‘mid’ point or ‘elbow’ will thereby identify a β_{opt} that reflects a surface slope characteristic common to the small spatial domain the method is applied to but possibly unique to a geographical region or latitude.” Further additions emphasizing the relation between physical characteristics and our methodological choices are described per specific comments from Reviewer 2 below.

Specific comments

P.2,L.7: What do you mean with ‘‘conventional input data’’. This should be a bit more elaborate.

By ‘‘conventional’’ we meant what the second half of the sentence describes. We have restructured the sentence to be more clear: ‘‘...requires input data that currently are, or are starting to become, freely available globally (hereafter referred to as ‘conventional’ data)’’

P. 2,L.25: I do not see that this reduction of D is correct. The ice cliff transect s oriented parallel to x, but D is the ice cliff width from bottom to top, which is in an angle (perpendicular) to x. In this case an integral 0-D by dx makes no sense

We believe we have corrected this error by defining D as the map view transect distance rather than the true distance in x,z space, this should allow a meaningful integration with respect to x: ‘‘a nadir looking sensor will capture the width of an ice cliff in map-view as, D , a distance that under represents the true distance from the bottom debris-ice interface to the top debris-ice interface by a factor of $\int_0^D \cos(\beta)dx$, where β is surface slope along the ice cliff transect, oriented parallel to the x -axis.’’

P.3,L.8/9: Could you clarify what ambiguities you mean? Your method only aims on slope, while radiometric sensors aim on roughness, brightness and temperature. There might be a range of possible ambiguities.

We have reworded the leading sentence for clarity and added a detailed example of a specific ambiguity: ‘‘A ‘‘thin’’ debris layer is undetectable from DEM data (with the possible exception of data with a spatial resolution that is sufficiently below the size of the rock clasts/fragments). With data at a sufficient resolution (dependent on clast size and abundance), ‘‘thin’’ debris can be detected by visible spectrum or thermal sensors which can both facilitate mapping this quantity but also possibly introduce ambiguities when defining ice cliff area. For example, if the same ice cliff is mapped from thermal data twice in the same (summertime) day, once at night (where, for this example, the ‘‘thin’’ debris is $< 0^\circ\text{C}$, in thermal equilibrium with the neighboring bare ice and is thus undetectable) and again midday (where the ‘‘thin’’ debris is the same, $> 0^\circ\text{C}$, temperature as the debris cover surrounding the ice cliff and classified as such), a single scientist might generate two very different maps of an ice cliff area that, in reality, experienced no significant chance.’’

P.3,L.6-20: This paragraph is rather unclear to me. Is there any relation to published observations? Based on my observations (of course depending on the definition of an ice cliff), cliff have no ability to accumulate any debris larger than small rock flakes. The temporal evolution of cliffs shows that coarse debris can accumulate at the bottom and slowly covers the cliff, but then it should not be considered a cliff anymore. As I mentioned in the introduction, in my opinion the definition of an ice cliff makes only sense if it is connected to the considerable difference in thermal fluxes. Therefore the geometry aspect is only a supporting approach.

We acknowledge that this paragraph might not have global applicability and have changed the leading sentence to reflect this: “A factor that may be abundant in some regions and add to the complexity of identifying and mapping ice cliffs is the presence of thin or sparse debris cover on an ice cliff face...”. With regard to whether this paragraph should be included at all, we point to Figures 3,5,7b,c,10 and 11 of this manuscript where debris cover on ice cliff faces on Canwell Glacier in Alaska is, we think, quite clear visually and quantified in Figure 7a. To our knowledge there are currently no published studies that discuss in detail ice cliffs in Alaska or North America. We hint at the question of whether abundant “thin” debris cover is specific to some regions, e.g. p.5 L.28 (location in original manuscript submission), but the focus of this article is mapping ice cliffs and the associated ambiguities. We leave this possibly interesting question of relative abundances of “thin” debris cover in different geographical regions to a future study.

P.3,L.24: Cliff slopes mainly differ due to aspect and thus solar radiation. There are several publications connected to this topic. It is likely that there is some overlap, but it is probably rather small, because what could be the physical reason that coarse debris sticks to one part of the slope, but it slides from the other part with the same angle? The only situation I can see is a small and short slope, where the talus is large enough to prevent additional mass movement from the steeper part.

We agree that a physical explanation of why there is overlap is lacking in this (mapping focused) manuscript and from our investigation. Any explanation would be speculative without a deeper process based study. However, both insert plots in Figure 3 show substantial overlap. Because the overlapping area (1) is substantial; (2) appears in DEM data from two different data acquisition sources; and (3) considerable care went into manually digitizing ice cliff area, we were convinced that the overlap is real and not entirely composed of error and/or inaccurate data.

P.3,L.29: The spatial resolution below 1m seems a random choice without any example from reality. You could provide some real observations about typical ice cliff height, slope and map view expression, to demonstrate which resolution is required to clearly capture ice cliffs.

We have rewritten the sentence and hope it adds some of the desired clarity: “While very high 1 m spatial resolution data capable of not only resolving ice cliff faces but clasts of surrounding

debris would be ideal for mapping confidence, data at this resolution are neither freely available or available at large scales (e.g. for a whole mountain range).”

P.3,L.31: Again the definition of conventional is missing.

Addressed in comment above and now defined on P.2 L.7.

P.3,L.32: 5m might be moderate for visible imagery, but for large coverage elevation data this is still high resolution.

We have removed the word ‘moderate’ here and throughout the manuscript.

P.4,L.23: High vertical accuracy is not critical for cliff localization, but for correct slope calculation, the relative accuracy is decisive.

Changed as suggested.

P.5,L.2: Can you shortly specify the data used for calibration already here?

Changed as suggested.

P.5,L.7: What do you mean with different surfaces? Types?

Changed as suggested.

P.5,L.13: can you provide some specifications about the data collection? Chip dimensions, mean flight elevation, ground resolution, spatial overlap?

Additions made as suggested with the exception of spatial overlap which is now mentioned but not quantified and we think that camera manufacturer and model are sufficient details for the purpose of this study, further camera specifications are easily found with this information. However if the Editor prefers these specifications be included we are happy to add them.

P.5,L.16: Again, can you please provide the spatial ground resolution?

Changed as suggested.

P.5,L.30-32: This sentence is difficult to understand. Do you mean the differences in the ice cliff slope distribution indicates that a unique value cannot be used for larger regions?

Changed to: “The shift between the two ice cliff slope distributions shown in the two inset histograms of Fig. 3 suggest that even if overlooking overlap errors, a simple surface slope threshold deemed suitable to define ice cliffs at one location may capture a different portion of the distribution in other regions on Earth.”

P.6,L.10: Is this an additional GeoEye scene (23rd December), compared to the one used before (29th December)? Please clarify.

Corrected. Thank you for catching this error.

P.6,L.23: what is an \area threshold"?

The sentence in question (“Bare ice below the area threshold (included as debris-covered area) that is not part of an ice cliff will be rejected as ice cliff area in the subsequent step based on low surface slopes.”) refers to the method mitigating patches of flat bare ice that are similar size to an ice cliff and surrounded by debris cover. This is probably a very minor nuance/technicality in the problem of mapping ice cliffs and we have removed the entire sentence.

P.6,L.27: As in many other cases, the manuscript would be more easily readable if expressions could be simplified: ‘‘elevation difference’’ instead of ‘‘rate of change in elevation’’. Please check also other cumbersome expressions

Changed as suggested.

P.7,L.21: what does ‘‘piecewise’’ mean in this context? This description is misleading. The iterative process is based on n iterations of varying beta. But the probability model is not ‘‘piecewise’’

We have removed the word “piecewise”.

P.8,L.6: The parameter of the probability map is $p(x)$ not beta. Maybe it could be written: ice cliff probability maps $p_i(x)$ in dependence of β_i .

Removed “ (β_i) ”.

P.8,L.7: see comment above about complicating the readability: \vector ice cliff cape area" basically means ‘‘the resulting ice cliff area’’

Changed as suggested.

P.8,L.11/12: This sentence does not explain the characteristics of the function in relation to the parameters: Why are the $y(\beta)$ are unrealistically high for low β ? $y'(\beta)$ approaches 0 for larger β s due to the nature of the exponential function. This is true for the existence of ice cliffs, but also without. It is rather a distinction that high β s do not occur, if there are no cliffs, because debris cannot be maintained on steep slopes

This section has been rewritten to better relate the method described to the physical setting. “The curve expresses unrealistically high $y(\beta)$ with low values of β because the threshold slope for ice cliff classification is well below slopes from surface roughness/undulations common for a debris-covered portion of a glacier. If there are ice cliffs within the spatial domain, the increase in β towards 90° causes the threshold to become too stringent, excluding even true ice cliff area. Steep ice cliff faces (and possibly erroneous DEM data) will cause iterations to run through high values of β with minor reductions in $y(\beta)$ causing the slope of $y(\beta)$, $y'(\beta)$, to gradually approach 0 as β approaches 90° . If there are no ice cliffs within the spatial domain, the iterative process will end as soon as $A_{cliff_i} = 0$ which will likely occur at a lower β relative to spatial domain with ice cliffs because debris cover can only be maintained on a subset distribution of surface slopes (see inset histograms in Fig. 3). This truncation is likely the key distinction of areas with no ice cliffs relative to ice cliff abundant domains (see Sect. 5.2).”

P.8,L.16: The formulation most accurate final A_{cliff} and coupled $p(x)$ is not necessarily true. It is probably the optimum combination of A_{cliff} and $p(x)$.

Changed as suggested.

P.8,L.22: please refer to Fig. 6 already here, so that the reader can relate this difficult description to the graphical expression

Reference added.

P.8, eq.4: what mathematical form should ‘‘distance (P1,P2,(beta, y(beta))) represent’’? This formulation seems strange. Can you give some indication how you came to the resulting right hand side of eq. 4?

Following “distance (P1,P2,(beta, y(beta)))” we give the expanded form of this shorthand. We describe the shorthand in the text: “ d is the orthogonal distance from a line defined by points P_1 and P_2 to the function $y(\beta)$ ” We are not sure who to cite for the distance from a point to a line equation.

P.9;l.5: It should already be mentioned here that γ has small thresholds.

Changed as suggested: “ γ is an input parameter with a near zero value (Table 1) defining...”

P.9,L.6: I do not see any problem with also calculating realistic values for P2 at beta=90°. Maybe it would be a better approach to use the point of inflexion of the gamma function as optimum. Because this is defined, based on the approximated parameters a, b and c only

Since the Reviewer cites parameters a, b, and c we assume she/he means the point of inflection of the function $y(\beta)$ (Eq. 2) rather than a gamma function. This was the initial approach we tried when designing the technique, however, the so-called 'elbow' point we were after can be found as an inflection only of a high order (4th) derivative which could be a mathematically unstable quantity. We therefore deemed it best to add an additional parameter with the hypothesis that it might be stable when applied in different regions on Earth.

P9,L.10: This is not an additional iteration, but a final application of the model with the found β_{opt} .

Changed as suggested.

P9.,L.11/12: Does this indicate that you just use a manual β_i if the methods fails? What would be the potential reasons for the method failing?

We added “manual[ly]” for clarity and added a sentence describing why we think the method could fail: “If visual inspection suggests large errors, all of the ice cliff probability maps and resulting ice cliff area shapefiles generated from the earlier set of iterations are retained and can be manually assessed to establish if a more adequate β_i value should be considered optimal. Future applications of this method that produce large errors might indicate that a fixed γ value is not suitable for all regions or that the surface slope distributions of debris covered area and ice cliff area have too much overlap to use surface slope alone as a deterministic attribute.”

P.9,L. 20: The fractional debris covered area represents the original classification of debris covered glacier, where embedded clean ice is included in the debris cover?

“(considering only debris-covered area)” was added to the first sentence of this section: “Using this method over large spatial domains might be computationally demanding on typical desktop or laptop computers. To address this, a precursory function segments large domains (considering only debris-covered area) into less computationally taxing tiles.”

P.10,L.6: The truth dataset x is probably different from the parameter x in $p(x)$. Can you explain?

It was intended to be the same, read as ‘probability that a pixel falls within x given β and ω . But we agree this was unclear. We have restructured this notation in a way that we believe is more correct. x is now defined as a pixel in the spatial domain and we solve for the probability that x =Ice cliff, given β and ω . We have removed all reference to the truth dataset being called x and describe it each time it is mentioned with words.

P.10,L.15: What is the secant of a slope pixel? Here it seems that you calculate a volume (length by area) instead of an area (length by length). Please reformulate.

We have rewritten the method description for finding true surface area and hope that is now more clear: “True surface area (as opposed to map view surface area) was calculated to present final results (Sect. 4 and 5.3) by multiplying DEM pixel area by a factor correcting for constant-sloped terrain ($\cos(\beta)^{-1}$, the secant of slope angle) for each pixel and finding the sum of slope corrected area for all ice cliff pixels or pixels within the entire spatial domain.”

P.10.L.19/20: Again please simplify: “‘tool output vector shape defined by A_{cliff} ’” means probably the same as “‘ A_{cliff} vector shapes’”.

Changed as suggested.

P.11,L.12: delete “‘for error distribution <1’”

Changed as suggested.

P.12,L.2: Can you comment here on the color coded distribution of ‘‘true positive’’ results in fig. 7? It seems there is a clear distinction in dependence of beta. What is the meaning of that?

We think that addressing this comment at P.13 L.12 is a location more on topic with the reviewers point. We have changed the sentence there to: “The figure shows a clear *true positive rate* dependence on slope illustrating the limitations of this method to detect ice cliffs where steep surface slopes were not sufficiently resolved in the data.”

P.12,L.9: magnitude (typo)

Correction made.

P.12,L.19: What would be the difference in this example of Fig. 6, using P_1 (β_i) for 60° and 90° ?

We apologise but do not completely follow this question or what changes/corrections might be implied. If P_1 is extended further from the position set by Eq. 5 the final ice cliff area would be less, in this way the method is sensitive to γ .

P.12,L.20/21: this needs more emphasis, that the truly artificial determination of β_{opt} from the Gaussian distribution matches with the error optimum based on the calibration.

Changed as suggested.

P.13,L.14/15: I do not understand this sentence. Can you please elaborate on the limitations with respect to slope angle?

Changed to: “The figure shows a clear *true positive rate* dependence on slope illustrating the limitations of this method to detect ice cliffs where steep surface slopes were not sufficiently resolved in the data.”

P.13,L.14: Low slope means that the spatial dimension of the cliff is so narrow that the elevation difference between pixels is dominated by the more flat debris covered parts. The cliff portion itself is still "steep". Beyond the ice cliff means, beyond the spatial classification result

This is what we meant by “...were not resolved in the data.” We added the word “sufficiently” and removed mention of the possible condition of a low surface slope ice cliff, we agree this is somewhat oxymoronic.

P.13,L.19: What means ‘‘surface slope may be saturated’’?

Drawing from the Reviewers comment above we changed this sentence to: “The abundance of small ice cliffs with a very low *true positive rate* shown in Fig. 7 indicate improvements to automated ice cliff detection will need to, in part, focus on small ice cliffs where the elevation difference between pixels might be dominated by the more flat surrounding debris-covered area and cause a dampening the steep ice cliff signal.”

P.15,L.11: The example of Figure 8 should be accompanied by the characteristics of the ice cliff results from Canwell Glacier, because the performance depends clearly on the typical ice cliff width and slope distribution.

Added: “With a coarsening of DEM resolution, larger ice cliffs were still correctly identified but with a loss of precision in ice cliff geometry and smaller ice cliffs dropped below the detection limit.”

P.15,L.17: There still exists a result for β_{opt} : about 19° and y_{opt} : about 4%. The only indication that the method fails is the non-assympotic shape of the fuction towards the x-axis? What is the reasoning behind this?

We had given this reasoning, following P.15,L.17: “A domain with ice cliffs will likely have at least a few very steep areas that will carry computations through higher values of β_i , while simple undulating surface topography should not produce abruptly steep slope values and as soon as β_i exceeds the maximum slope present, iterations will stop. ” but have rewritten this in an effort to be more precise: “While there is likely a range of slopes where debris-covered area and ice cliff area will both exists (inset histograms in Fig. 3), ice cliffs, by definition, are steep features that will carry iterations towards 90° . If this ice cliff component is not present,

the iterations will terminate as soon as there is no longer area with a slope above the slope threshold for a given iteration. This termination is a key characteristic that could indicate there are no ice cliffs within the spatial domain (Fig. 9).”

P.15,L.29: What is meant with ‘‘mass wasting’’? Is it removal of supra-glacial debris? Mass wasting usually is used for ice loss

“(geomorphic)” added before “mass wasting”.

Fig. 5: Panel (e) is not mentioned on the caption.

Panel (e) description has been added.

Automated detection of ice cliffs within supraglacial debris cover

Sam Herreid and Francesca Pellicciotti

Department of Geography, Faculty of Engineering and Environment, Northumbria University, Newcastle upon Tyne, UK

Correspondence to: Sam Herreid (samherreid@gmail.com)

Abstract. Ice cliffs within a supraglacial debris cover have been identified as a source for high ablation relative to the surrounding debris-covered area. Due to their small relative size and steep orientation, ice cliffs are difficult to detect using nadir-looking space borne sensors. The method presented here uses surface slopes calculated from digital elevation model (DEM) data to map ice cliff geometry and produce an ice cliff probability map. Surface slope thresholds, which can be sensitive to geographic location and/or data quality, are selected automatically. The method also attempts to ~~included~~include area at the (often narrowing) ends of ice cliffs which could otherwise be neglected due to signal saturation in surface slope data. The method was calibrated in the Eastern Alaska Range, Alaska, USA, against a control ice cliff dataset derived from high resolution visible and thermal data. Using the same input parameter set that performed best in Alaska, the method was ~~applied~~tested against ice cliffs manually mapped in the Khumbu Himal, Nepal. Our results suggest the method can accommodate different glaciological settings and different DEM data sources without a data intensive (high resolution, multi-data source) re-calibration.

1 Introduction

Ice cliffs are steep, bare-ice surface features that can develop within a debris-covered portion of a glacier. The direct atmosphere-ice interface can result in significantly higher ablation rates relative to the surrounding debris-covered area and are therefore areas of interest when solving for glacier melt in heavily debris-covered regions (Buri et al., 2016b; Thompson et al., 2016; Brun et al., 2016). The mechanism(s) of ice cliff formation, the controls of ice cliff migration patterns and ice cliff residence time on a glacier are gaining research attention but are still poorly understood processes ~~and a present~~, in part, due to a lack of base data ~~is an obstacle to establishing a robust understanding~~ (Reid and Brock, 2014; Watson et al., 2017). Melt and surface energy fluxes at specific ice cliffs have been studied in detail (Sakai et al., 1998; Han et al., 2010; Sakai et al., 2002; Reid and Brock, 2014; Buri et al., 2016a) and digital elevation model (DEM) differencing has shown the spatial trends of enhanced glacier melt relative to surrounding debris cover and ice cliff evolution at the scale of several cliffs or a single glacier tongue (Thompson et al., 2016; Brun et al., 2016). All of the studies mentioned suggest that ice cliffs, if present ~~within a debris cover~~on a debris-covered glacier, need to be accounted for in order to adequately model glacier mass change and response to climate. A wide range of ice cliff abundance within a ~~debris covered~~debris-covered area is possible, from no ice cliffs to an abundance capable of possibly negating, or even reversing, the net melt reducing effect of surrounding debris cover (Kääb et al., 2012; Basnett et al., 2013; Gardelle et al., 2013).

To the knowledge of the authors, five methods have been used to map ice cliffs: (1) field mapping (e.g. Steiner et al., 2015); (2) manual digitization from remote sensing data (e.g. Sakai et al., 1998; Han et al., 2010; Thompson et al., 2016; Watson et al., 2017); (3) automatically, using a surface slope threshold (e.g. Reid and Brock, 2014); (4) automatically by a principal component analysis using visible near infrared and shortwave infrared satellite bands (Racoviteanu and Williams, 2012); and (5) automatically by a object based image analysis of unmanned aerial vehicle data (Kraaijenbrink et al., 2016). None of the remote sensing studies listed offer a confidence metric based on independent data for their ice cliff map products and field mapping is not realistic for large-scale analysis.

The objective of this paper is to present a new approach to automate the detection of ice cliffs. The method (1) requires ~~conventional~~ input data that ~~are currently are, or are~~ starting to become, freely available globally (hereafter referred to as 'conventional' data); (2) automatically selects threshold values that can accommodate varying surface textures (e.g. glacier area with a characteristically smooth debris cover or a characteristically rough/hummocky debris cover); and (3) is assessed for quality against additional high resolution visible and thermal data.

1.1 Formulation of the problem

The importance of ice cliffs has become increasingly clear (Sakai et al., 1998; Han et al., 2010; Sakai et al., 2002; Watson et al., 2017), but the mapping of these features remains a challenge, especially at spatial scales beyond a few glaciers. The map-view surface expression of an ice cliff is often a crescent, circular or linear swath of steep, bare (or thinly debris covered) glacier ice surrounded by a debris layer. Steep glacier ice not completely surrounded by debris cover might exhibit melt and evolution patterns similar to ice cliffs, but the lack of a bounding debris cover makes these areas characteristically distinct from ice cliffs and are thus excluded in this study. It is unclear at the present time if a small area of low angle (i.e. not cliff) bare glacier ice ~~enclave within a debris cover~~ located within a debris-covered portion of a glacier or a narrow swath of ice constrained by debris cover (e.g. a narrowing gap between two widening medial moraines) should be considered similar to ice cliffs with respect to relative melt rates in a debris-covered environment, but for this study we maintain a focus on identifying only steep features.

Watson et al. (2017) report that most ice cliffs within a subset of glaciers in the Central Himalaya are 200 m or less in length with a length of 20-40 m being the most frequent. Thompson et al. (2016) report a mean ice cliff height of 15.5 m ~~for at~~ Ngozumpa Glacier in Nepal with notable outliers up to ~45 m. No current literature suggest other glacierized regions on Earth have ice cliffs with dimensions that deviate wildly from these localized findings. Due to this relatively small size and the high slope angle of an ice cliff, a nadir looking sensor will capture ~~map-view ice cliff width as~~ the width of an ice cliff in map-view as, D , the a distance that under represents the true distance from the bottom debris-ice interface to the top debris-ice interface ~~;~~ reduced by a factor of $\int_0^D \cos(\beta) dx$ by a reduction factor of $\int_0^D \cos(\beta) dx$, where β is surface slope along the ice cliff transect, oriented parallel to the x -axis (to simplify this example formulation). This (likely) narrow map-view area means that even in an ideal situation where there is no debris on an ice cliff face, the optically sharp boundary between rock and ice could be saturated or completely muted in remote sensing data where ice cliff area does not occupy a sufficient fraction of a data pixel. A DEM-derived surface slope expression of an ice cliff is not encumbered by debris cover on the cliff face, yet the 'true' steep slopes of an ice cliff can also be saturated or completely muted if the spatial resolution of the computed slopes ~~is~~ are coarse to

a point where no slope value is calculated solely from pixels located within an ice cliff face. For both visible and DEM data, in the common case where an ice cliff narrows gradually at the cliff ends, ice cliff edge defining signal saturation is likely to increase towards the narrow ends and could cause a systematic underestimation of ice cliff area if left unaccounted for.

5 If cloud free, ablation season visible spectrum imagery is used to map ice cliffs, cliff aspect, surrounding topography and sun position at the time of data acquisition control whether the surface will be shaded or illuminated. North and south facing ice cliffs ~~will likely be optically distinct and crescent to~~ present in a single image will likely appear either dark (shaded bare ice) or light (illuminated bare ice) relative to unshaded surrounding debris cover. Crescent to circular ice cliffs will likely exhibit a spectrum of shade and illumination. Automated or manual ice cliff mapping techniques using cloud free visible spectrum imagery would likely need to mitigate this factor and ~~devise a way to discriminate between shadowed~~ also discriminate between
10 shaded ice cliff area and ~~shadowed~~ shaded debris-covered area.

~~An important factor pertaining to~~ A factor that may be abundant in some regions and add to the complexity of identifying and mapping ice cliffs is the presence of thin or sparse debris cover on an ice cliff face (hereafter referred to as a “thin” debris cover, ~~although also but still~~ describing sparse debris cover that could include large clasts or boulders). A “thin” debris layer is ~~completely undetectable from moderate resolution DEM data and can introduce ambiguities if identifying~~ undetectable from
15 DEM data (with the exception of data with a spatial resolution that is sufficiently below the size of the rock clasts/mapping ice cliffs from visible spectrum or thermal imagery. The surface of fragments). With data at a sufficient resolution (dependent on clast size and abundance), “thin” debris can be detected by visible spectrum or thermal sensors which can both facilitate mapping this quantity but also possibly introduce ambiguities when defining ice cliff area. For example, if the same ice cliff is mapped from thermal data twice in the same (summertime) day, once at night (where, for this example, the “thin” debris
20 is $< 0^{\circ}\text{C}$, in thermal equilibrium with the neighboring bare ice and is thus undetectable) and again midday (where the “thin” debris is the same, $> 0^{\circ}\text{C}$, temperature as the debris cover surrounding the ice cliff and classified as such), a single scientist might generate two very different maps of an ice cliff area that, in reality, experienced no significant change. The “thin” debris covering an ice cliff face during the melt season can vary with the deposition and/or removal of rock fragments. This process could be a slow evolution (e.g. coupled with melt, neighboring sediment distributions and englacial debris concentration) or
25 a near instantaneous result from a local storm (e.g. windblown silt accumulations on wet, rough ice cliff surfaces). These processes lead to an ambiguity in defining an ice cliff where time may need to be considered. For example, if an image of a cliff shows that 30% of the surface area within the cliff face is comprised of large rocks caught on narrow ice ledges, should this area be excluded from what is called an ice cliff or can it be assumed this debris cover is transient and superfluous to consider? At large scales, a time consideration of debris cover within ice cliff faces is unrealistic, yet a 30% error could have a large and
30 compounding impact on, for example, a study calculating energy fluxes. Furthering this example to the case where over time a cliff face is 100% debris covered, there are two classification possibilities: the cessation of being an ice cliff or, if the cliff exhibits some unique signature (e.g. a thermal anomaly and/or fine sediment/clast size distribution relative to the surrounding debris cover), it could still be considered an ice cliff.

Considering the cessation case where ice cliff area transitions to ~~debris-covered area in the wider context of non-ice cliff~~
35 ~~yet~~ steep debris-covered glacier area(e.g. the side of a medial moraine)area, it is not unrealistic that the true distributions of

a population of ice cliff surface slopes and a population of debris-covered area surface slopes will have some overlap. If true, this implies that a simple surface slope threshold alone cannot cleanly identify ice cliff area.

5 A highly successful automated or manual ice cliff mapping technique will likely require a combination of multiple input datasets (e.g. visible and thermal data or visible and elevation data) yet still, ambiguities with defining what is and is not an ice cliff will likely remain regardless of approach.

~~Ultimately, the leading obstacle to successfully identifying ice cliffs is data resolution and quality. Data with a spatial resolution. While very high <1 m are spatial resolution data capable of not only resolving ice cliff faces but clasts of surrounding debris would be ideal for mapping ice cliffs, however, at the present time, confidence, data at this resolution are often not freely available, particularly neither freely available or available at large scales (e.g. whole mountain ranges).~~

10 ~~With an effort for a whole mountain range). Considering this, we attempted~~ to balance ice cliff identification success rate with input data that is conventional and becoming freely available at wide spatial scales,~~the.~~ The automated method presented here uses ~~moderate-resolution (.17ex5 m)~~ digital elevation data alone to identify ice cliffs. The method includes a procedure to identify ice cliff area at the ends of ice cliffs that have a narrowing end geometry. <1 m resolution visible imagery collected in the Alaska Range are used to assess the abundance of “thin” debris cover on ice cliff faces.

15 2 Data

2.1 Input data

There are three required datasets for this method: (1) the glacier area over which the method is applied; (2) multispectral satellite imagery; and (3) a ~~moderate-resolution DEM~~ DEM with .17ex~5 m resolution. Since the DEM alone is used to identify ice cliffs (the likely most temporally transient feature ~~considered~~ present in the data), it is not crucial that all three
20 data sets be coincident in time. However, debris-covered area and glacier margins should be assessed to ensure they have not changed significantly over the time span of the data used.

2.1.1 Glacier area

The spatial domain over which ice cliffs are detected is bound by a user defined polygon. The perimeter can outline a portion of a glacier, a whole glacier or many glaciers and can be a mix of debris covered and debris free glacier area. A subset of the
25 Randolph Glacier Inventory (Pfeffer et al., 2014) is a suitable input but should be assessed for accuracy to avoid any erroneous inclusion of off glacier slopes which could be misidentified as ice cliff area and skew computed statistics. Computational cost might become a factor for typical desktop or laptop computers if solving over a large domain. This issue is addressed in Sect. 3.3.

2.1.2 Satellite imagery

Multispectral satellite imagery is only used [in this method](#) to map debris cover. The ratio of a near infrared (NIR) band and a shortwave infrared (SWIR) band is used to empirically remove radiance value variance from topographic illumination angles and, to some degree, cast shadows (Vincent, 1973). Data from the NASA/USGS Landsat program (used in this study) and ESA
5 Sentinel-2 are two data sources that meet the input spectral and resolution requirements to map debris cover and are freely available.

2.1.3 DEM

Elevation data are key in both identifying the location of ice cliffs and also defining their area. For the results of the method to be meaningful, an input DEM must have sufficient resolution and precision to resolve topography below or near the size of
10 most ice cliffs within an area of interest. Because ice cliff locations are not being identified as the residual of DEM differencing, a high vertical accuracy [relative to the geoid](#) is not critical ([while relative vertical accuracy is decisive](#)). This can simplify data processing if structure from motion data are used to derive the input DEM. Photogrammetric methods are often ~~very~~ successful at resolving ~~vertical precision (i.e. relative topography)~~ and [relative topography and image correlation methods simplify](#) geolocation in x, y ~~is usually simple to achieve~~, but a high vertical accuracy with respect to the geoid (i.e. true elevation)
15 requires a suitable ground control point network (Westoby et al., 2012).

DEM data that meet this criteria are not freely available for all glacierized regions on Earth at the present time. However, initiatives such as the Interagency Arctic Research Policy Committee (IARPC) Arctic DEM, which is releasing a freely available 2 to 8 m resolution DEM for all landmass above 60° and the entire State of Alaska, show promise that high resolution DEM data may soon be available globally.

20 2.2 Calibration and validation data

The parameters of this method were calibrated using [manually derived ice cliff outlines based on high resolution visible \(.17ex~8 cm\) and thermal \(80 cm\)](#) data that cover a portion of the Canwell Glacier in the Eastern Alaska Range, Alaska, USA. To test transferability, the same parameter set was applied to a portion of Ngozumpa Glacier in the Khumbu Himal, Nepal [with an independent validation dataset previously published in Thompson et al. \(2016\)](#).

25 2.2.1 Canwell Glacier

Canwell Glacier (Fig. 1, 2a) is a 60 km², northwest flowing glacier in the eastern Alaska Range (63° 19.8'N, 145° 32'W). Canwell Glacier was selected for this study because several different ~~surfaces~~ [surface types](#) exist in close proximity: an expansive ice cliff network in debris cover that transitions, orthogonal to flow, to bare glacier ice and a medial moraine.

On the 29th of July, 2016 between 11:00 and 11:16 local Alaska Time, nadir (or near-nadir) looking visible and thermal
30 infrared images were collected from a helicopter over ~~1.7~~ [1.74](#) km² of the Canwell Glacier capturing all of the different surface types listed above (Fig. 3a). The images were collected below a high overcast ceiling. This caused subtle cloud effect to be

captured by varying light penetration of the cloud layer, however, this also removed the likely more negative effect of shading discussed in Sect. 1.1. 250 visible spectrum images were collected with a Canon EOS 70D camera ~~These at an altitude range of about 133-615 m above the glacier surface. Overlap between these~~ images, in conjunction with 9 ground control points, were used to generate a ~8 cm resolution orthomosaic and a 1 m resolution (resampled to 5 m to match a spatial resolution more common from space borne sensors) DEM using the proprietary software Agisoft PhotoScan Professional Edition. 34 (suitable for use) thermal images were collected with a FLIR T620 camera and processed using the proprietary software FLIR Tools. Emissivity was held constant at 0.95, atmospheric temperature and relative humidity were measured from the helicopter during image acquisition using a Kestrel 4000 Weather Meter and distance from the sensor to the glacier surface was estimated using camera locations derived by Agisoft Photoscan. The thermal images were manually georeferenced to match the orthomosaic image described above and has a uniform, resampled spatial resolution of 80 cm.

A nearly cloud-free Landsat 8 image was acquired over the Canwell Glacier (path/row: 67/16) on the 31st of August, 2016. Debris cover extent and glacier margins were found to be effectively static over the 33 day interval between the acquisition of helicopter-borne and Landsat 8 data.

2.2.2 Ngozumpa Glacier

15 Ngozumpa Glacier (Fig. 1, 2b) is a 60 km² south flowing glacier in Khumbu Himal (27° 57'N, 85° 42'E). Ngozumpa Glacier was selected ~~for to be used in~~ this study for two reasons, ~~first,~~ First, it is located in a ~~distinctly different geographical location with a debris cover that is typical of the Himalaya and~~ geographical region that is different from the Alaska Range with respect to latitude, longitude, continentality, climate and orogeny. These factors and others establish a setting where exposure to the sun, the overall debris cover (e.g. debris extent, clast sizes, thickness) and glacier dynamics at Ngozumpa Glacier is notably different from ~~the~~ Canwell Glacier. Fig. 3 illustrates some differences between Canwell and Ngozumpa glaciers including rock/boulder size, ice cliff size, amount of “thin” debris cover on ice cliff faces and overall hummocky nature of the debris-covered area. The debris on Ngozumpa Glacier is thick (1-3 m towards the terminus (Nicholson, 2005)) and covers the full width of the glacier continuously for nearly the entire ablation zone. ~~Differences-~~

The shift between the two ice cliff slope distributions shown in the two inset histograms ~~in-of~~ Fig. 3 suggest that even if overlooking overlap errors, a simple surface slope threshold deemed suitable to define ice cliffs at one location ~~cannot be assumed to have wide reaching applicability~~ may capture a different portion of the distribution in other regions on Earth. The second reason Ngozumpa Glacier was selected is that an automated ice cliff map can be assessed against the manually generated ice cliff map from Thompson et al. (2016), allowing the removal of some potential manual delineation bias in this study.

30 Thompson et al. (2016) provided their GeoEye-1 orthoimage acquired on the 29th-23th of December, 2012, the corresponding stereo image derived DEM (1 m resolution, resampled to 5 m for this study) and their ice cliff map generated manually using both the orthoimage and DEM. Additionally, Thompson et al. (2016) generated and provided a mask of area where surface elevation was poorly resolved. The method Thompson et al. (2016) used to map ice cliffs was to define a line along the top edge of each ice cliff based on optical characteristics and steep surface slopes calculated from the DEM. In order to

conduct a quality assessment between the top edge lines defined by Thompson et al. (2016) and the automated ice cliff polygons identified using the method presented here, the ice cliff top edges from Thompson et al. (2016) were manually adjusted to polygons incorporating the area of each ice cliff using the December 23rd, 2012 visible GeoEye-1 imagery. Some smaller ice cliff additions were also made.

5 A nearly cloud-free Landsat 8 image was acquired over Ngozumpa Glacier (path/row: 140/41) on the 30th of November, 2014. Because the portion of Ngozumpa Glacier considered in this study is 100% debris covered, a debris extent map generated with a 2 year gap does not alter the spatial domain. The glacier margin was mapped from the December 23rd, 2012 GeoEye-1 imagery.

3 Methods

10 3.1 Isolation of debris-covered area

The spatial domain is refined from total glacierized area, including bare ice and accumulation zone area, to only debris-covered glacier area. Debris-free area is identified and removed using the band ratio of NIR and SWIR satellite bands with a user defined threshold (Paul et al., 2004)(Table 1). To prevent the removal of bare ice pixels that are part of an ice cliff, closed shapes identified as bare ice within the debris-covered area are filled (reclassified as debris-covered area) if below a user
15 defined threshold area (Table 1). This is possible where an ice cliff is debris-free and big enough to cause one or more satellite image pixels to fall below the NIR/SWIR ratio threshold. ~~Bare ice below the area threshold (included as debris-covered area) that is not part of an ice cliff will be rejected as ice cliff area in the subsequent step based on low surface slopes.~~

3.2 Ice cliff identification

3.2.1 Iterative ice cliff detection

20 Within debris-covered area, surface slope (β), is calculated as the maximum ~~rate of change in elevation~~ elevation difference for each DEM pixel value relative to its 8 neighbor values. A threshold slope value β_i , isolates steeper area from which statistics and further threshold values are derived. ~~The tool~~ This area, and all subsequent areas derived in the mapping method, are simplified as a shape in two dimensions (2D). Only final results of the mapping method are converted to 3D surfaces (Sect. 4 and 5.3, method described in Sect. 3.4 used synonymously with 'true surface area' and 'area considering slope'). The method
25 is run iteratively, varying β_i over the full range of possible surface slopes (below over-vertical), from 0 to 90° in n iterations (i).

For each i , two areas are defined that will, together, define area with a high likelihood of being an ice cliff: (1) an initial ice cliff area (A_i) from which statistics are computed, further geometries are derived and the base shape of the final ice cliff area is defined; and (2) A_{ei} , an area slightly more encompassing than A_i from which lengthwise ends of the final ice cliff geometries
30 are extracted (subscript 'e' for 'end').

A_i is defined as $area(\beta > \beta^*_i)$ where $\beta^*_i = mean(\beta > \beta_i)$ (Fig. 4a). Using β^*_i rather than simply β_i speeds up computation by discarding the case where ice cliffs occupy an overwhelming percentage ($>>50\%$) of the debris-covered area. If ice cliffs did occupy one half or more of a debris-covered area (in map-view), its classification as a debris-covered portion of a glacier could be questioned.

5 Ice cliff centerlines are computed by creating a Voronoi cell for each vertex in the outline of A_i converted to a dense set of vertices. The bounding edges of each Voronoi cell is removed except for the edge in the center of a shape in A_i . A point removal line simplification is applied to smooth extraneous bends, particularly at centerline ends. The centerline ends are then extended by a user defined distance, L_e (Fig. 4b), with the topological restriction that centerline extensions can intersect, but not cross one another (Fig. 4b). The extended centerlines are then transformed to an area, B_{ei} , by a buffer distance, α , applied outward in all directions (Fig. 4b). C_{ei} is the intersection of B_{ei} and A_{ei} , where A_{ei} is area with a surface slope greater than β^*_i relaxed by a user defined factor, β_e (Fig. 4c). C_{ei} is intended to identify area that is part of an ice cliff but expressed by surface slopes less than β^*_i due, possibly, to narrowing ice cliff ends where DEM data and subsequent surface slope calculations saturate a true, steep surface slope signal. Area with a high likelihood of being an ice cliff, A_{cliff_i} , is defined as the union of C_{ei} and A_i where a user defined minimum shape area threshold, A_{min} is exceeded (Fig. 4d).

15 A_{cliff_i} is the definitive ice cliff area used for the error analysis in Sect. 3.5 after optimization described in Sect. 3.2.2, but for some applications of this method, a distributed probability map might be a more useful product. With β_i as a lower limit and β_u , where $\beta_u = \beta^*_i + std(\beta > \beta_i)$, as an upper limit, ~~a piecewise probability model can be defined as-~~

20 ~~Where the probability of each pixel being part of a true ice cliff~~ the probability that a pixel, x , is part of an ice cliff can be estimated where

(1) From

Eq. ??, ice cliff probability is assigned given surface slope, β , and ω , where ω is a binary classification ~~$\{Y, N\}$~~ $\{1, 0\}$ for pixels falling within A_{cliff_i} , ~~$Y=1$~~ , and outside A_{cliff_i} , ~~$N=0$~~ . For pixels where ~~$\omega = N = 0$~~ , ice cliff likelihood is reduced by a user defined factor, φ . $\varphi = 0$ implies the iterative process will have zero error, $\varphi = 1$ discards the entire iterative process and $\varphi = 0.5$ (for example) means that a surface slope $> \beta_u$ but not bound by a high likelihood ice cliff shape (A_{cliff_i}) will be assigned a ~~$p(x|\beta, \omega)$~~ $p(x = Ice\ cliff | \beta, \omega)$ value of 0.5. With this use of $\varphi = 0.5$ as a reduction factor, area iteratively identified as ice cliff will ~~have a $p(x|\beta, \omega)$~~ be assigned a $p(x = Ice\ cliff | \beta, \omega)$ that is a factor of 0.5 greater than any other area but no steep surface slope will be completely rejected as having ~~$p(x|\beta, \omega) = 0$~~ $p(x = Ice\ cliff | \beta, \omega) = 0$.

The result of this iterative process is $90/n$ gridded ice cliff probability maps and vector ice cliff shapes (A_{cliff_i}) for the entire spatial domain.

3.2.2 Heuristic selection of β_{opt} : a best β_i

The $90/n$ ice cliff probability maps (β_i) are constrained by two conditions: where the spatial domain is unrealistically dense with ice cliff and where there is zero ice cliff area. Using the vector ice cliff shape resulting ice cliff area (A_{cliff_i}), ice cliff fraction, y_i , is calculated as $A_{cliff_i}/area(spatial\ domain)$. To derive a continuous, functional form of ice cliff fraction, a

5 single-tailed ($\beta \neq 0$) Gaussian distribution function, the equation

$$y(\beta) = a \exp\left(-\left(\frac{\beta - b}{c}\right)^2\right), \quad (2)$$

is fit to y_i and β_i using non-linear least squares where a , b and c are fitting parameters. The curve expresses unrealistically high $y(\beta)$ with low values of β and, if ice cliffs do exist because the threshold slope for ice cliff classification is well below slopes from surface roughness/undulations common for a debris-covered portion of a glacier. If there are ice cliffs within the

10 spatial domain, the increase in β towards 90° causes the threshold to become too stringent, excluding even true ice cliff area. Steep ice cliff faces (and possibly erroneous DEM data) will cause iterations to run through high values of β with minor reductions in $y(\beta)$ causing the slope of $y(\beta)$, $y'(\beta)$, approaches to gradually approach 0 as β approaches 90° . If there are no ice cliffs within the spatial domain, the curve will reach $y(\beta) = 0$ without a long tail (ending further iterations iterative process will end as soon as $A_{cliff_i} = 0$, which will likely occur at a lower β relative to spatial domain with ice cliffs because debris

15 cover can only be maintained on a subset distribution of surface slopes (see inset histograms in Fig. 3). This truncation is likely the key distinction of areas with no ice cliffs relative to ice cliff abundant domains (see Sect. 5.2). If there are ice cliffs within the spatial domain, some value of β_i will best match optimize a match with the true ice cliff fraction. The method uses a heuristic approach to select this β_i , termed β_{opt} , which might provide the most accurate final A_{cliff} and coupled $p(x|\beta, \omega)$

$p(x = Ice\ cliff | \beta, \omega)$ map.

20 Where β is low and $y(\beta)$ is unrealistically high, all ice cliffs will likely be included (high *true positive rate* [defined in Sect. 3.5]) yet will be accompanied by a large amount of non-ice cliff area (low *precision* [defined in Sect. 3.5]). Conversely, as β approaches 90° , or $max(\beta)$ if $max(\beta) < 90^\circ$, the small areas within $y(\beta)$ will very likely be ice cliff area (high *precision*), but widely under resolve the true ice cliff area. In the absence of validation data to explicitly optimize *true positive rate* and *precision*, the ‘mid’ point or ‘elbow’ of the curve as $y(\beta)$ shifts from a steep slope, high $y'(\beta)$, to $y'(\beta)$ approaching 0, is

25 hypothesized to correspond to the optimized maximum of both *true positive rate* and *precision* -(Fig. 6). The hypothesis is that as β_i increases and less sloped debris-covered area (e.g. from strain and differential melt) is included as mapped ice cliff, true ice cliffs will begin to comprise the majority of the mapped ice cliff fraction (y_i). We hypothesize this to have a stabilizing effect (ice cliffs are a small, consistently steep area), lowering the rate of loss of mapped ice cliff area and slope of the curve as β_i continues towards 90° . We hypothesize that this so-called ‘mid’ point or ‘elbow’ will thereby identify a β_{opt} that reflects a

surface slope characteristic common to the small spatial domain the method is applied to but possibly unique to a geographical region or latitude. This point, (β_{opt}, y_{opt}) is defined as

$$(\beta_{opt}, y_{opt}) = (\beta, y(\beta)) \text{ where } (\beta, y(\beta)) \cap \max(d), \quad (3)$$

where

$$d = \text{distance}(P_1, P_2, (\beta, y(\beta))) = \frac{|(y_2 - y_1)\beta_i - (\beta_2 - \beta_1)y + \beta_2 y_1 - y_2 \beta_1|}{\sqrt{(y_2 - y_1)^2 + (\beta_2 - \beta_1)^2}}. \quad (4)$$

d is the orthogonal distance from a line defined by points P_1 and P_2 to the function $y(\beta)$ (Eq. (2)), where

$$\begin{aligned} P_1 &= (\beta_1, y_1) \\ \beta_1 &= \beta \text{ where } y'(\beta) = \gamma \\ y_1 &= y(\beta_1) \end{aligned} \quad (5)$$

and

$$\begin{aligned} P_2 &= (\beta_2, y_2) \\ \beta_2 &= \beta \text{ where } y(\beta) = \max(y(\beta)) \\ y_2 &= y(\beta_2). \end{aligned} \quad (6)$$

10 γ is an input parameter with a near zero value (Table 1) defining the limit when $y'(\beta)$ is effectively 0. Since the function asymptotically approaches 0, without γ , β_1 would always be 90° and this geometric approach would likely fail to identify the so called ‘mid’ point or ‘elbow’ of the curve. Additionally, DEM errors can sometimes have vertical or near vertical slopes (e.g. a raised artifact). These errors will be identified as ice cliff area but will not impede the calculation of (β_{opt}, y_{opt}) because very steep area causes a vertical translation of the function $y(\beta)$, thus not affecting $y'(\beta)$.

15 ~~Finally, the iterative method is again run for one more iteration~~ A final application of the model where $\beta_i = \beta_{opt}$ ~~to produce~~ produces a final automated ice cliff probability map. If visual inspection suggests large errors, all of the ice cliff probability maps and ~~vector ice cliff shapes resulting ice cliff area shapefiles~~ generated from the earlier set of iterations are retained and can be manually assessed to establish if a more adequate β_i value should be considered optimal. Future applications of this method that produce large errors might indicate that a fixed γ value is not suitable for all regions or that the surface slope distributions
20 of debris covered area and ice cliff area have too much overlap to use surface slope alone as a deterministic attribute.

3.3 Domain segmentation for large areas

Using this method over large spatial domains might be computationally demanding on typical desktop or laptop computers. To address this, a precursory function segments large domains (considering only debris-covered area) into less computationally taxing tiles. Because the ice cliff mapping depends on statistics calculated across the entire area considered, it is critical that

5 ~~no segment be small so that statistics cannot be meaningfully~~ segments are large enough so that meaningful statistics can be computed. A target/maximum spatial domain is defined by the user as the length of an edge of a square, L_t . If the debris covered area of interest is below L_t^2 , no segmentation will be applied. If the debris covered area is greater than L_t^2 , the debris covered area is subdivided by a square grid with side length L_t . The function finds the area of debris cover occupying each grid cell and attempts to merge neighboring cells one at a time until their fractional debris-covered area sum to 1. A

10 look distance factor in number of $L_t \times L_t$ cells, n_c , controls if and how far the ~~tool-method~~ will look beyond empty space or cells where an unsuccessful match (summed fraction > 1) occurred and still be considered as ‘neighboring’ cells. When a cell or set of previously merged cells have (1) exhausted the set of possible neighboring cells within the look distance, and (2) all have returned a summed debris cover fraction greater than 1, the cell or set of cells are defined as a closed tile that will become an input spatial domain to the iterative and heuristic optimization scheme. The ~~tool-method~~ automatically identifies

15 and individually processes each tile and a final merged product of both gridded ~~$p(x|\beta,\omega)$~~ $p(x = Ice\ cliff|\beta,\omega)$ and a vector shapefile corresponding A_{cliff} are generated.

3.4 Derivation of a calibration dataset for Canwell Glacier

To calibrate a method that automatically maps ice cliff area, a sufficiently accurate ‘truth’ dataset, ~~x~~ , is needed. ~~We define x as the area defined manually by digitizing~~ For this study, ice cliff outlines generated from the high resolution visible and thermal

20 data described in Sect. 2.2.1 were considered to be true. Elevation data described in Sect. 2.2.1 were not explicitly used to digitize from but were used in a 3D viewer with draped visible and thermal layers to assess generated ice cliff outline quality. Area that was clearly ice cliff in visible and thermal data but not apparent in elevation data (possibly due to errors in the DEM) was still mapped as ice cliff area. Given the ambiguities described in Sect. 1.1 regarding “thin” debris cover, ice cliffs were liberally outlined, including, for example, cliffs that were nearly 100% covered by debris, yet had a unique thermal signature

25 relative to the surrounding debris cover indicating thinner debris. No minimum size was considered, thus ice cliffs below the resolution of the ~~tool-method~~ input data are penalized in quality assessment metrics, if missed. While we made an effort to manually map ice cliffs based on consistent criteria, there is subjective interpretation within this ‘truth’ dataset. We did not quantify the uncertainty associated with this subjectivity.

True ~~ice-cliff~~ surface area (area considering slope, as opposed to map view surface area) was calculated ~~by summing~~

30 to present final results (Sect. 4 and 5.3) by multiplying DEM pixel area by a factor correcting for constant-sloped terrain ($\cos(\beta)^{-1}$, the secant of slope ~~pixels derived from DEM data within x and multiplying by the area of a DEM pixel angle) for each pixel and finding the sum of slope corrected area for all ice cliff pixels or pixels within the entire spatial domain.~~

3.5 Statistical measures of performance

A suite of statistical measures of performance are needed to isolate and illustrate performance trade-offs and rank success between parameter sets and alternative, less complex methods. All performance metrics are calculated using the ~~tool-output~~ vector shape defined by final output ice cliff area A_{cliff} rather than distributed ~~$p(x+\beta, \omega)$~~ $p(x = Ice\ cliff | \beta, \omega)$. True positive

- 5 (TP) is defined as area where the ice cliff mapping technique output intersect true ice cliff area, ~~x~~ . True negative (TN) is defined as area where the method did not identify ice cliffs that intersects true non-ice cliff area (debris-cover area), ~~x^c~~ . False positive (FP) and false negative (FN) are defined as area identified as ice cliff that is not included in ~~x~~ the manually defined 'true' ice cliff map and ice cliff area present in ~~x~~ the manual map but absent in the automated output, respectively. Using these quantities, the following common metrics (e.g. Fawcett, 2006) are defined:

10 $true\ positive\ rate = \frac{TP}{TP + FN}$ (7)

$$precision = \frac{TP}{TP + FP} \quad (8)$$

$$accuracy = \frac{TP + TN}{TP + FP + FN + TN}. \quad (9)$$

- $True\ positive\ rate$ (also called recall) is the ratio of successful classification over total true ice cliff area and $precision$ measures the probability that area identified as ice cliff is in fact ice cliff. Ideally, these metrics should be equal to each other and, if the cliff mapping is perfect, both equal 1. $Accuracy$ is the proportion of true results, but because ice cliffs will most often occupy a small fraction of a debris-covered area and $accuracy$ accounts for TN as well as TP , it becomes a less informative metric. For example, if 1% of a debris-covered portion of a glacier is ice cliff, not mapping ice cliffs at all will yield an ice cliff mapping $accuracy$ of 99%. We therefore introduce two additional metrics, outside of the standard suite of statistical measures of performance, that are independent of TN and thus help evaluate ice cliff mapping success:
- 15

20 $error\ distribution = \frac{FP}{FN}$ (10)

$$error\ magnitude = \frac{FP + FN}{TP + FN}. \quad (11)$$

$Error\ distribution$ provides a measure of balance between FP and FN errors. An $error\ distribution > 1$ means there is more debris-covered area mapped erroneously as ice cliff than ice cliff area erroneously mapped as debris-covered and

vice versa ~~for error distribution < 1~~ . Ideally, *error distribution* is 1. *Error magnitude* is a ratio of the total erroneously mapped area, both FP and FN , over the ~~true manual 'true'~~ ice cliff area (~~x~~ , which is equal to the sum of TP and FP). If *Error magnitude* is 0 ice cliffs are perfectly mapped, if *error magnitude* is, for example, 2, then error is a factor of 2 greater in spatial extent than the true ice cliff area.

5 3.6 Calibration

The method presented here requires five key input parameters to map ice cliffs: L_e , α , β_e , A_{min} and γ (Table 1, described in Sect. 3.2.1, bold font quantities in Fig. 4). A matrix of different parameter sets were tested using Canwell Glacier data. The success of each parameter set was quantified against the manually generated ice cliff outlines described in Sect. 3.4 using the statistical measures of performance derived in Sect. 3.5.

10 3.7 Quantification of “thin” debris cover on ice cliffs

As described in Sect. 1.1, ice cliffs can be considerably covered by rock fragments. The automated method presented here uses elevation data alone and therefore depends on the assumption that steep terrain within a debris cover is ice cliff. Because the validation data described in Sect. 3.4 is in part visible data, assessment of “thin” debris cover on ice cliffs can be made and used to further interpret automated ice cliff mapping results. Here, the word “thin” is used colloquially under the premise that an ice surface able to retain large clasts and/or a debris cover equal or greater in thickness (and surface temperature) to the surrounding debris-covered area is not an ice cliff, leaving dust to small clasts to constitute “thin” debris covering on ice cliff faces. The optical orthomosaic was converted to greyscale and a pixel value threshold was selected manually that discriminated between debris-free and debris-covered area. We did not quantify the sensitivity of this threshold parameter and relied on visual assessment (e.g. comparing panels b and c to panels d and e in Fig. 7) to determine a single values that minimized errors (e.g. due to varying lithology)and maximize success. This process is similar to the satellite data based method described in Sect. 3.1 to identify debris-covered area, but without a band ratio correction and at a much higher spatial resolution of ~ 8 cm. The results provide an estimate of the distribution and fraction of debris cover on ice cliffs and is shown (Fig. 7).

4 Results

4.1 Canwell Glacier

25 The manually generated, ‘true’ ice cliff dataset ~~x~~ , shows 4.9% of the ~~1.7~~1.74 km² Canwell Glacier study area is ice cliff in map view (not considering slope). Ice cliff map view area (84,630 m²) under represents true ice cliff surface area (104,920 m², considering slope) by 19%. Considering the true surface area of the Canwell Glacier study area, map view under represents true surface area (1.86 km²) by 6%. Considering both true surface area of ice cliffs and the Canwell Glacier study area, the fraction of ice cliff area is 5.7%.

Table 2 shows the [automated mapping method](#) parameter set matrix described in Sect. 3.6. The results summarized in Table 2 (1) suggest that the method is stable and robust because no parameter set produced exceptionally poor results (e.g. computed ~~error magnitude~~ [error magnitude](#) across all parameters sets fall within a range of 0.94 to 1.06); and (2) allow the selection of a ‘best’ parameter set, selected with an emphasis on high and equal values of *true positive rate* and *precision*: $L_e = 10$ m, $\alpha = 3.54$ m, $\beta_e = 3^\circ$ and $A_{min} = 250$ m². γ is excluded from Table 2 because after testing different values of γ , a value of 0.0001 consistently returned results where *true positive rate* and *precision* are close to equal. Calibration results in Table 2 are shown alongside the same statistical measures of performance applied to a range of simple surface slope thresholds used to identify ice cliffs. This comparison shows that a carefully selected slope threshold can provide an ice cliff map comparable in statistical measure to the more complex method presented here. However, simple slope threshold results are shown to be sensitive with respect to the slope value used and would require additional data, similar in quality to those described in Sect. 3.4, to validate the threshold selection and subsequent results.

Using the parameter set [$L_e = 10$ m, $\alpha = 3.54$ m, $\beta_e = 3^\circ$, $A_{min} = 250$ m² and $\gamma = 0.0001$] as input, Fig. 6 shows the heuristic approach for selecting β_{opt} , a best β_i . ~~While the location of (β_{opt}, y_{opt}) is dependent on γ and therefore not mathematically robust, the close coincidence of β_{opt} is calibrated so that there is close coincidence between β_{opt} and β where~~ *true positive rate* and *precision* intersect (Fig. 6) ~~suggests the technique performs as intended~~. *Error magnitude* deviated only slightly from a value of 1 in all of the parameter set tests. This indicates the best results of this method are incurring errors equal in area to the true area of ice cliffs. This is a non-trivial error but likely an unavoidable trade off for a method designed for wide scales and modest data input. It is important to note that comparing only percent ice cliff area values between ~~measured, \approx manually mapped ice cliffs,~~ (4.9%), and modeled (5.3%) would give a misleading perception of very low error, 0.4%, when the true error is closer to 5% ($1 - accuracy$) if considering the entire domain or higher if considering only ice cliff area error (*true positive rate* and *precision*). For most tests, errors are fairly distributed between FP and FNs and shown by *error distribution* having a proximity to 1. As described in Sect. 3.5, *accuracy* is a poor indicator of success mapping a feature that occupies a small fraction of a total area, favoring a setting of higher *precision* over *true positive rate*, but it is the only metric used in this study that rewards *TN* area and quantifies overall performance.

Results using the best parameter set for Canwell Glacier have an *accuracy* of 0.952, where *FP* and *FN* errors are close to evenly distributed with an *error distribution* = 1.14 and an *error magnitude* = 0.98, which is slightly below the mean for all tested parameter sets (0.99). *True positive rate* and *accuracy* are higher (0.54 and 0.51, respectively) than those achieved by the best simple slope threshold, 27° (0.49 and 0.50, respectively). These results suggest that the method presented here can achieve results that are slightly more accurate than the best simple slope threshold and is far more robust: sensitivity to changing parameters is low while different simple slope threshold values produce wider variance in statistical measures of performance (Table 2) and are thus more sensitive.

4.1.1 Mapping success in the context of ice cliff characteristics

Figure 7 shows mean surface slope, map view surface area and the percentage of “thin” debris covering every ~~ice cliff mapped in \approx manually mapped ice cliff~~. These characteristics are shown in the context of *true positive rate* (Eq. (7)) now calculated

for every ice cliff (*true positive rate* mentioned in all instances prior was calculated for all ice cliffs together), and *FP* ice cliffs, which we define as isolated shapes that are solely *FP* area and do not share a boundary with a shape in ~~the manually mapped ‘true’ ice cliff area~~. The figure shows ~~a clear true positive rate dependence on slope illustrating the limitations of this method to detect ice cliffs where steep surface slopes were not sufficiently resolved in the data. The figure shows~~ that, in this portion of Canwell Glacier, most of the “cleanest” ice cliffs are still covered by a non-trivial (>50%) amount of debris. The percentage of “thin” debris cover on ice cliff faces appears continuous above 50%, such that there is no clear boundary in the data that could define what is and is not an ice cliff if the percentage of “thin” debris cover was the main deterministic variable.

~~Figure 7 provides a wider context to what is present in reality and what is detected as an ice cliff by the automated method presented here. The figure shows the limitations of detecting ice cliffs where steep surface slopes are either not present or not resolved in the data.~~

4.2 Ngozumpa Glacier

Table 3 shows the performance of the best parameter set found for Canwell Glacier applied to the lower ablation zone of Ngozumpa Glacier (4.8 km²). There is a decrease in performance, for example, *true positive rate*, *precision* and *error magnitude* for Canwell Glacier are 0.54, 0.51 and 0.98, respectively, and 0.53 (−1%), 0.32 (−19%) and 1.58 (+0.6), respectively, for Ngozumpa Glacier. The imbalance between *true positive rate* and *precision* indicates the automatically selected β_{opt} does not coincide with the ideal β_i where *true positive rate* and *precision* are optimized. However, in the context of ~~the simple slope threshold results shown in Table 3, β_{opt} was off by only $\pm 2.5^\circ$ the best possible threshold is 39° (*true positive rate and precision constrained between simple surface slope thresholds 35° and 40°) the statistical measures of performance from the automated method are closest to a simple slope threshold of 37° . This suggests that the automated method missed selecting optimum threshold(s) by about 2° .* Considering that not a single alteration was made to the ~~model input parameters method and input parameter values used for Canwell Glacier~~, the method mitigated the ~~different surface type (very hummocky surface relative to Canwell Glacier, see many physical differences between Canwell and Ngozumpa glaciers (described in Sect. 2.2.2 and shown in Fig. 3) and as well as different DEM generation method methods (satellite based rather than airborne structure from motion) far better than~~. This ability to accommodate different physical characteristics enables the method to outperform a simple slope threshold found at ~~Canwell Glacier and assumed to be transferable to one location, e.g. at Canwell Glacier, and assume that it is transferable to other places on Earth, e.g.~~ Ngozumpa Glacier (Tables 2 and 3). The debris covered area considered on Ngozumpa Glacier was broken into three processing tiles where β_{opt} found for each tile was 30.8° , 32.5° , and 33.5° , while β_{opt} for Canwell Glacier was 23.5° . The $\sim 10^\circ$ difference between β_{opt} for both glaciers is significant but appropriate for each location as shown in Fig. 3 or observed by comparing the statistical measures of performance for the range of simple slope threshold values shown in the far right column of Tables 2 and 3. Taking the best simple slope threshold of 27° found for Canwell Glacier and applying it to Ngozumpa Glacier would result in an ice cliff map with a *precision* of 0.10 (−41% relative to Canwell Glacier results) and area mapped incorrectly a factor of 7.91 (+6.93) times greater than the true ice cliff surface area (Table 3). Using the method presented here and the parameters from Canwell Glacier, *true positive rate* and *precision*~~

are closer to balanced and erroneously mapped area is only a factor of 1.58 greater than the true ice cliff area, comparable in magnitude (+0.6) to the best results for Canwell Glacier.

The results shown in Table 3 were generated without removing area identified in Thompson et al. (2016) as having poorly resolved surface elevation. Poorly resolved on-glacier area was predominantly at locations that were shaded by cast shadows and thus often concurrent with steep terrain and ice cliffs. Visual inspection of the data suggested that while the computed precision might be low, the well resolved area above and below steep terrain combined with the absence of extreme outliers resulted in steep terrain still being resolved as steep. Acknowledging the uncertainties within this context, we also ~~testing~~ tested the method with poorly resolved elevation locations removed from both the DEM and the manually generated ‘true’ ice cliff area. These results produced a reduction in *true positive rate* (0.44) yet more in balance with *precision* (0.38) and a comparable *error magnitude* (1.62).

5 Discussion

This method attempts to resolve two key components in DEM-based automated ice cliff mapping that are apparent in the histogram in Fig. 3: (1) selecting a threshold that discriminates between ice cliff and debris covered area; and (2) adding/removing the correct area that is within the surface slope overlap between ice cliff and debris-covered areas. The method presented here attempts to add low slope ice cliff area by looking beyond the ends of the ice cliffs and rejects area with the same (low) slope that is not neighboring the ends of an ice cliff. Rejecting area that is steep but not truly ice cliff is difficult using elevation data alone. The only mechanism to remove this area within this method is eliminating mapped ice cliff area below a ~~threshold,~~ however minimum area threshold; however, this is a delicate balance between reducing errors and reducing resolution to which the ~~tool method~~ can resolve ice cliffs. The abundance of small ~~,low-angle~~ ice cliffs with a very low *true positive rate* shown in Fig. 7 indicate improvements to automated ice cliff detection will need to, in part, focus on small ice cliffs ~~whose surface slope may be saturated due to data resolution~~ where the elevation difference between pixels might be dominated by the more flat surrounding debris-covered area and cause a dampening the steep ice cliff signal.

5.1 Alternative approach

Alternative methods were tested before selecting the presented method as best. One alternative approach used optical satellite data to accept or reject potential ice cliff area. A main objective in this approach was identifying and removing the *FP* ice cliffs clustered at the top of Fig. 7. The Landsat 15 m panchromatic band was corrected for illumination variance from topography using the Minnaret method (Smith et al., 1980). Bright and dark regions of the image were then identified as area $mean(L_H) \pm std(L_H)m$ where L_H is Minnaret corrected radiance values and m is a model parameter. These regions were established with the assumption that ice cliffs with an aspect that is illuminated by the sun would be optically bright relative to surrounding debris cover and ice cliffs with an aspect that is in cast shadow would be optically dark relative to surrounding debris cover. A buffer sequence was then applied to separate shapes that were narrowly attached (e.g. hourglass shaped): shapes were uniformly shrunk and expanded by a user defined distance. A shape that contained $area > 0$ of both seed slope area (e.g.

$area > \beta_u$ [β_u is defined in Sect. 3.2.1]) and optically bright or dark area would be assigned a high ice cliff likelihood. However, this method failed to perform better than a method using surface slopes alone because of two linked factors: data resolution and “thin” debris covering true ice cliffs. Figure 7 shows that even the “cleanest” ice cliffs are still around 50% debris covered. A 15 m optical pixel perfectly centered on an ice cliff with 50% debris cover should have a distinguishable signal, but this is a best case in both pixel/ice cliff location coincidence and fraction of “thin” debris cover. It is clear to see how using 15 m resolution data will quickly fail to resolve smaller and more debris-covered ice cliffs. The buffer sequence to separate narrowly attached shapes had the positive (intended) result of detaching narrowly joined debris-covered area and ice cliff area, allowing ice cliff area to be considered separately and positively identified as an ice cliff while rejecting the debris covered area. However, the shrinking step had the negative (and more frequent) effect of completely removing shapes that where, in at least one dimension, equal to or less than $2 \times$ the user defined buffer distance.

5.2 Wider application

The testing of this method at two locations on opposite sides of the Earth with the same input parameters suggests the method can be applied/transferred elsewhere with little loss of performance. Figure 8 shows repeat runs for the Canwell Glacier with all parameters ~~constant only held constant while~~ resampling the DEM to different resolutions. With a coarsening of DEM resolution, larger ice cliffs were still correctly identified but with a loss of precision in ice cliff geometry and smaller ice cliffs dropped below the detection limit. This offers a first order estimate of how performance will decline with coarsening DEM data resolution; however, it is possible that a recalibration of the input parameters could improve results when using data at lower resolutions.

To examine how this method performs for a debris-covered area with no ice cliffs, TP and FP area was removed from the Canwell Glacier spatial domain. Because FP area is already identified as area where the ~~tool-method~~ fails, we removed this area also so that all remaining area is ice cliff free with maximum confidence. Figure 9 shows the resulting plot for selecting β_{opt} . The method still ~~(erroneously) identified produced a resulting map of~~ ice cliffs; however, the shape of $y(\beta)$ abruptly terminates rather than slowly approaching zero. ~~This is the key characteristic that would suggest there are actually no ice cliffs within the spatial domain. A domain with ice cliffs will likely have at least a few very steep areas~~ While there is likely a range of slopes where debris-covered area and ice cliff area will both exist (inset histograms in Fig. 3), ice cliffs, by definition, are steep features that will carry ~~computations through higher values of β_i , while simple undulating surface topography should not produce abruptly steep slope values and iterations towards 90° . If this ice cliff component is not present, the iterations will terminate~~ as soon as ~~β_i exceeds the maximum slope present, iterations will stop~~ there is no longer area with a slope above the slope threshold for a given iteration. This termination is a key characteristic that could indicate there are no ice cliffs within the spatial domain (Fig. 9). Due to the abrupt termination of the curve derived where no ice cliffs are present in reality, a high measure of linear correlation, e.g. Pearson correlation coefficient (r), between β_i and y_i might offer an automated binary classification of whether a spatial domain does or does not contain ice cliffs. Further testing would be required to derive a threshold value that could be confidently applied to other data, but the data shown in Fig. 9 supports this hypothesis where $r = -0.98$ for a spatial domain with no ice cliffs and $r = -0.91$ for a spatial domain with ice cliffs.

5.3 What are ice cliffs and how should glaciologists map them?

Throughout this paper the ambiguity of what is an ice cliff has been mentioned. Figure 10 shows an example of an area possibly in the process of becoming an ice cliff. The relief of this medial moraine has facilitated a setting where [\(geomorphic\)](#) mass wasting exceeded englacial debris exhumation and accumulation. The area remains evenly and largely debris-covered, but does appear distinct both in visible and thermal imagery. However, if this is considered sufficient criteria to be defined as an ice cliff, there is no clear edge where ice cliff ends and debris cover begins. We had a difficult time deciding if this feature should be included in the ~~'truth' dataset~~ [\(x\) 'true' ice cliff dataset](#), ultimately deciding to include it (and similarly ambiguous features), but also with the caveat in Sect. 3.4 stating that "ice cliffs were liberally outlined". The slope of the feature identified in Fig. 10 was sufficient to be identified by the automated method as an ice cliff while the surrounding slopes of the medial moraine were not.

Figure 11 shows a second example where an ice cliff could be mapped in detail excluding bands of debris within the ice cliff face (Fig. 11d) or could be mapped more broadly including the debris bands (Fig. 11c). This is a setting where time could be considered when defining an ice cliff as described in Sect. 1.1. If these debris bands are long term fixtures and there are sufficient data to resolve the individual ice cliff faces then possibly the detailed mapping is correct. However, if the clasts within the debris bands are transported to the ice cliff margins and not resupplied the more broad/coarse mapping approach would be appropriate. For this study, we delineated ice cliff(s) 1 from Fig. 11 using the more coarse mapping approach.

While higher resolution data capturing a suite of properties (e.g. visible and surface temperature data) can further resolve what is truly present, it will likely not resolve classification ambiguities (e.g. Fig. 10 and 11), and at the present time these data are not available at large scales. Focus should therefore be more targeted towards mapping consistency. This is best met when automated methods can be applied with sufficient levels of confidence, eliminating technician bias and error.

For both automated and manual mapping methods used [this study in this study](#), we map ice cliffs as a 2D area ~~or~~ [\(or converted to a 3D surface\)](#). An alternative method to map ice cliffs is to define a line along the ice cliff top edge (e.g. Thompson et al., 2016; Watson et al., 2017). Figure 11 provides a comparison of all three methods (3D surface area, 2D map view surface area and 1D top edge line) and shows that when mapping ice cliffs as a 2- or 3D area, refined detail leads to a refined (smaller/more accurate) area, while refined detail leads to an expansion of ice cliff top edge length when mapping ice cliffs in 1D. This suggests that 2- or 3D area is a more reliable measure and likely more communicative if drawing a comparison with other areas or regions or studies.

6 Conclusions

This study presents a new automated method for mapping ice cliffs within supraglacial debris cover. The method uses glacier outlines and satellite imagery to isolate debris-covered area where ice cliffs might exist and then uses DEM data alone to map ice cliff area. The DEMs used in this study had a spatial resolution of 5 m. The method is designed to accommodate regional variability in ice cliff characteristics by selecting unique surface slope threshold values automatically. The method also attempts to improve performance by explicitly considering the often narrowing ends of ice cliffs. The method was calibrated using

data from Canwell Glacier in Alaska, USA, and validated using data from Ngozumpa Glacier in Nepal. The best parameter set for Canwell Glacier produced an ice cliff map with essentially equivalent success to a carefully selected simple surface slope threshold, which itself carried a degree of error with *true positive rate* and *precision* both around 0.5. While the application of a simple surface slope threshold is a much easier mapping technique, the selection of a sufficient threshold requires supplemental, high resolution data due to the rapid increase in error with less ideal threshold selections. The method presented here ~~reduces attempts to automatically mitigate~~ this instability and ~~offers more offer a~~ confident ice cliff ~~mapping map~~ when supplemental data are not available. With no parameter alteration, the method was applied on the other side of the world. Results from Ngozumpa Glacier show a decrease in performance relative to Canwell Glacier where *true positive rate* is similar but *precision* is 19% less. This is still however, an ice cliff map with more success than if the carefully selected simple surface slope threshold for Canwell Glacier was assumed to be transferable to Ngozumpa ~~glacier~~ Glacier. Under this assumption, *precision* is 41% less and the ice cliff area mapped incorrectly is a factor of 6.93 more than the results for Canwell Glacier. We therefore conclude that simple surface slope thresholds (1) carry a non trivial degree of error even if carefully selected; and (2) cannot be considered to be transferable to other regions. In this study we have quantified (1) and presented a method to mitigate (2).

While we only consider two locations, these results offer an idea of how well the method might perform in other regions without supplemental validation data and opens the possibility for deriving ice cliff area at large scales. With a DEM of adequate spatial resolution, which we show is best if around 5 m, and sufficient computational capacity, this ~~tool~~ method could be applied to all glacierized area on Earth. Additionally, ~~running the tool on~~ applying the method to temporal data will produce a time-lapse evolution of ice cliff formation, cessation, melt patterns and motion through the glacier flow regime. Further validation of this method using ice cliff maps from high resolution visible, thermal or other data in other regions will help to either support or discredit our claim of wide applicability. Ambiguities defining what is an ice cliff are likely to persist in any technique used to map ice cliffs, but map variance from these ambiguities will become less of a factor if a consistent methodology is used.

7 Code availability

~~pending publication~~ Code from this study is available within the Python/ArcPy(ArcGIS) ensemble Debris Cover Tools, which ~~are open source~~ is open source and available at <https://github.com/samherreid>.

Acknowledgements. This work was supported by a studentship from Northumbria University. The Technology Advisory Board at the University of Alaska Fairbanks provided funding for the FLIR thermal camera and the Canon camera was provided on loan by the University of Alaska Fairbanks Rasmuson Library. We thank Rebekah Tsigonis for her help in the field, Alex Shapiro at Alaska Land Exploration, LLC for saving us from having to bike all of the science gear into the Alaska Range, Sarah Roeske for letting us helicopter hitchhike alongside her fieldwork, Sarah Thompson for sharing her data and ice cliff map from Ngozumpa Glacier, Jed Brown and Markus Holzner for their help with mathematics and Ben Brock for his support early in the project ~~and Markus Holzner for his clever solution to an optimization problem.~~

References

- Basnett, S., Kulkarni, A. V., and Bolch, T.: The influence of debris cover and glacial lakes on the recession of glaciers in Sikkim Himalaya, India, *Journal of Glaciology*, 59, 1035–1046, 2013.
- Brun, F., Buri, P., Miles, E. S., Wagnon, P., Steiner, J., Berthier, E., Ragetti, S., Kraaijenbrink, P., Immerzeel, W. W., and Pellicciotti, F.:
5 Quantifying volume loss from ice cliffs on debris-covered glaciers using high-resolution terrestrial and aerial photogrammetry, *Journal of Glaciology*, 62, 684–695, 2016.
- Buri, P., Miles, E. S., Steiner, J. F., Immerzeel, W. W., Wagnon, P., and Pellicciotti, F.: A physically based 3-D model of ice cliff evolution over debris-covered glaciers, *Journal of Geophysical Research: Earth Surface*, 2016a.
- Buri, P., Pellicciotti, F., Steiner, J. F., Miles, E. S., and Immerzeel, W. W.: A grid-based model of backwasting of supraglacial ice cliffs over
10 debris-covered glaciers, *Annals of glaciology*, 57, 199–211, 2016b.
- Citterio, M. and Ahlstrøm, A.: The aerophotogrammetric map of Greenland ice masses, *The Cryosphere*, 7, 445, 2013.
- Fawcett, T.: An introduction to ROC analysis, *Pattern recognition letters*, 27, 861–874, 2006.
- Gardelle, J., Berthier, E., Arnaud, Y., and Kaab, A.: Region-wide glacier mass balances over the Pamir-Karakoram-Himalaya during 1999–2011 (vol 7, pg 1263, 2013), *Cryosphere*, 7, 1885–1886, 2013.
- 15 Han, H., Wang, J., Wei, J., and Liu, S.: Backwasting rate on debris-covered Koxkar glacier, Tuomuer mountain, China, *Journal of Glaciology*, 56, 287–296, 2010.
- Kääb, A., Berthier, E., Nuth, C., Gardelle, J., and Arnaud, Y.: Contrasting patterns of early twenty-first-century glacier mass change in the Himalayas, *Nature*, 488, 495–498, 2012.
- Kraaijenbrink, P., Shea, J., Pellicciotti, F., de Jong, S., and Immerzeel, W.: Object-based analysis of unmanned aerial vehicle imagery to map
20 and characterise surface features on a debris-covered glacier, *Remote Sensing of Environment*, 186, 581–595, 2016.
- Nicholson, L.: Modelling melt beneath supraglacial debris: implications for the climatic response of debris-covered glaciers, Ph.D. thesis, University of St Andrews, UK, 2005.
- Paul, F., Huggel, C., and Kääb, A.: Combining satellite multispectral image data and a digital elevation model for mapping debris-covered glaciers, *Remote sensing of Environment*, 89, 510–518, 2004.
- 25 Pfeffer, W. T., Arendt, A. A., Bliss, A., Bolch, T., Cogley, J. G., Gardner, A. S., Hagen, J.-O., Hock, R., Kaser, G., Kienholz, C., et al.: The Randolph Glacier Inventory: a globally complete inventory of glaciers, *Journal of Glaciology*, 60, 537–552, 2014.
- Racoviteanu, A. and Williams, M. W.: Decision tree and texture analysis for mapping debris-covered glaciers in the Kangchenjunga area, Eastern Himalaya, *Remote Sensing*, 4, 3078–3109, 2012.
- Reid, T. and Brock, B.: Assessing ice-cliff backwasting and its contribution to total ablation of debris-covered Miage glacier, Mont Blanc
30 massif, Italy, *Journal of Glaciology*, 60, 3–13, 2014.
- Sakai, A., Nakawo, M., and Fujita, K.: Melt rate of ice cliffs on the Lirung Glacier, Nepal Himalayas, 1996, *Bull. Glacier Res*, 16, 57–66, 1998.
- Sakai, A., Nakawo, M., and Fujita, K.: Distribution characteristics and energy balance of ice cliffs on debris-covered glaciers, *Nepal Himalaya, Arctic, Antarctic, and Alpine Research*, pp. 12–19, 2002.
- 35 Smith, J., Lin, T. L., Ranson, K., et al.: The Lambertian assumption and Landsat data, *Photogrammetric Engineering and Remote Sensing*, 46, 1183–1189, 1980.

- Steiner, J. F., Pellicciotti, F., Buri, P., Miles, E. S., Immerzeel, W. W., and Reid, T. D.: Modelling ice-cliff backwasting on a debris-covered glacier in the Nepalese Himalaya, *Journal of Glaciology*, 61, 889–907, 2015.
- Thompson, S., Benn, D. I., Mertes, J., and Luckman, A.: Stagnation and mass loss on a Himalayan debris-covered glacier: processes, patterns and rates, *Journal of Glaciology*, pp. 1–19, 2016.
- 5 Vincent, R. K.: Spectral ratio imaging methods for geological remote sensing from aircraft and satellites, *Proceedings of Symposium on Managment and Utilization of Remotely Sensed Data*, American Society of Photogrammetry, Sioux Falls, SD, October, pp. 377–397, 1973.
- Watson, C. S., Quincey, D. J., Carrivick, J. L., and Smith, M. W.: Ice cliff dynamics in the Everest region of the Central Himalaya, *Geomorphology*, 278, 238–251, 2017.
- 10 Westoby, M., Brasington, J., Glasser, N., Hambrey, M., and Reynolds, J.: ‘Structure-from-Motion’ photogrammetry: A low-cost, effective tool for geoscience applications, *Geomorphology*, 179, 300–314, 2012.

Table 1. Model parameters. Where β^*_i is the surface slope threshold that defines the basic ice cliff shape (A_i for each iteration, A_{e_i} is the same as A_i but with a slightly lower surface slope threshold, $p(x|\beta, \omega) - p(x = \text{Ice cliff} | \beta, \omega)$ is ice cliff probability given surface slope and overlap with A_{cliff} (Sect. 3.2.1), and $y(\beta)$ is the fraction of ice cliffs within the spatial domain as a function of surface slope. Look distance is the number of $L_t \times L_t$ cells the routine will look beyond and still consider as ‘neighboring’ during segmentation of a spatial domain greater than L_t^2 .

Symbol	Description	Value used in this study
	NIR/SWIR threshold for debris mapping (for this study: Landsat 8 OLI5/OLI6)	1.2
	Threshold area for bare ice area reclassified as debris-covered area	2700 m ²
n	Number of iterations	36 (2.5° increments over 90°)
L_e	Ice cliff centerline extension length	see Table 2
α	Centerline buffer distance	see Table 2
β_e	Degrees by which β^*_i is reduced to define A_{e_i}	see Table 2
A_{min}	Minimum ice cliff area threshold	see Table 2
φ	$p(x \beta, \omega) - p(x = \text{Ice cliff} \beta, \omega)$ reduction factor	0.5
γ	Limit where $y'(\beta)$ (derivative of Eq. (2)) is effectively 0	0.0001
L_t	Target/maximum domain processing square tile side length	1500 m (area: 2.25 km ²)
n_c	Look distance for domain segmentation	1

Table 2. Model parameter calibration at Canwell Glacier using statistical measures of performance derived in Sect. 3.5. The set of two boxes on the left describe what values are presented throughout the table and their ideal values. *True positive rate* is abbreviated here as *TP rate*. A well performing parameter set will have values of *true positive rate* and *precision* that are as close to 1 as possible and balanced. The middle set of boxes show performance for varying parameter sets. DEM resolution for this study was 5 m, thus variation of A_{min} was tested at 0, 5 and 10 pixels; L_e at $2\times$ and $4\times$ pixel length; and α at $(\text{pixel length} * \sqrt{2})/2$ and $\text{pixel length} * \sqrt{2}$. The set of boxes on the right show performance of simple surface slope threshold mapping of ice cliffs. Values in bold font are the highest ranking parameter sets for both the method described in this paper and the simple surface slope threshold method. Values in blue and red are the best and worst values, respectively, for all boxes in the table.

		$A_{min} = 0 \text{ m}^2$	$A_{min} = 125 \text{ m}^2$	$A_{min} = 250 \text{ m}^2$		
$L_e = 10 \text{ m}$		0.52 0.53	0.53 0.52	0.51 0.51		
	$\alpha = 3.54 \text{ m}$	0.954	0.954	0.953		
	$\beta_e = 3^\circ$	0.94	1.02	0.98		
$L_e = 20 \text{ m}$		0.52 0.53	0.51 0.53	0.51 0.50	20°	0.79 0.24
	$\alpha = 3.54 \text{ m}$	0.954	0.954	0.951		0.866
	$\beta_e = 3^\circ$	0.98	0.91	1.06		12.20
$L_e = 10 \text{ m}$		0.54 0.50	0.53 0.51	0.54 0.51	25°	0.60 0.41
	$\alpha = 7.07 \text{ m}$	0.952	0.952	0.952		0.938
	$\beta_e = 3^\circ$	1.14	1.10	1.14		2.22
$L_e = 20 \text{ m}$		0.54 0.50	0.54 0.50	0.54 0.50	27°	1.28
	$\alpha = 7.07 \text{ m}$	0.951	0.951	0.951		0.49 0.50
	$\beta_e = 3^\circ$	1.22	1.16	1.21		0.952
$L_e = 10 \text{ m}$		0.53 0.51	0.52 0.52	0.51 0.53	30°	0.97
	$\alpha = 3.54 \text{ m}$	0.953	0.953	0.954		0.34 0.66
	$\beta_e = 5^\circ$	1.08	1.02	0.93		0.960
$L_e = 20 \text{ m}$		0.51 0.51	0.53 0.51	0.50 0.51	35°	0.26
	$\alpha = 3.54 \text{ m}$	0.952	0.952	0.953		0.83
	$\beta_e = 5^\circ$	0.98	0.99	0.97		0.03 0.75
$L_e = 10 \text{ m}$		0.56 0.49	0.55 0.49	0.54 0.50	40°	0.956
	$\alpha = 7.07 \text{ m}$	0.950	0.950	0.951		0.04
	$\beta_e = 5^\circ$	1.32	1.29	1.16		0.91
$L_e = 20 \text{ m}$		0.56 0.47	0.56 0.48	0.55 0.48		0.03 0.75
	$\alpha = 7.07 \text{ m}$	0.948	0.949	0.950		0.952
	$\beta_e = 5^\circ$	1.43	1.40	1.29		0.01
		1.06	1.06	1.03		0.98

TP rate	Precision
Accuracy	
Error distribution	
Error magnitude	
1.00	1.00
1.000	
1.00	
0.00	

Table 3. Statistical measures of performance for Ngozumpa Glacier. The value arrangement is the same as in Table 2. The lone box on the left is the bold parameter set from Table 2 applied to Ngozumpa Glacier. The set of boxes on the right show performance of simple surface slope threshold mapping of ice cliffs ([at an interval of 5° with additional thresholds of interest \(Sect. 4.2\)](#)). Values in bold font are the highest ranking parameter sets for both the method described in this paper and the simple surface slope threshold method. Values in blue and red are the best and worst values, respectively, for all boxes in the table. The performance of a simple surface slope threshold at 27° is shown to discredit the possible assumption that the best threshold from Canwell Glacier (Table 2) could have wider applicability to other glaciers.

	$A_{min} = 250 \text{ m}^2$		0.94	0.05
$L_e = 10 \text{ m}$	0.53	0.32	0.596	
$\alpha = 7.07 \text{ m}$	0.980		264.34	
$\beta_e = 3^\circ$	2.38		16.21	
			0.89	0.08
			0.749	
			88.50	
			10.07	
			0.85	0.10
			0.803	
			53.41	
			7.91	
			0.79	0.14
			0.873	
			23.15	
			5.12	
			0.61	0.27
			0.949	
			4.20	
			2.03	
			0.52	0.35
			0.964	
			1.98	
			1.43	
			0.44	0.45
			0.973	
			0.95	
			1.10	
			0.40	0.50
			0.975	
			0.67	0.67
			1.00	
			0.26	0.70
			0.979	
			0.15	
			0.85	
			0.16	0.77
			0.978	
			0.06	
			0.89	

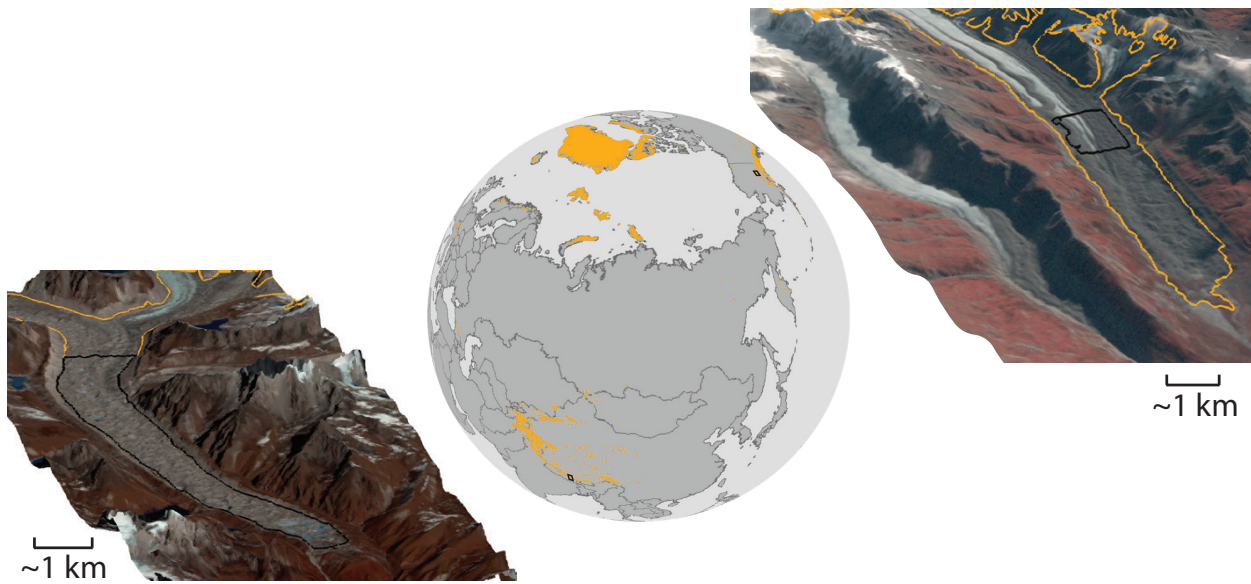


Figure 1. Location of Ngozumpa Glacier in the Khumbu Himal, Nepal ([left](#)) and Canwell Glacier in the Eastern Alaska Range, Alaska, USA ([right](#)). Global ice cover (Pfeffer et al., 2014; Citterio and Ahlstrøm, 2013) is shown in orange. In the oblique inset maps, orange lines are the glacier extent and the black polygons define the spatial domains used in this study. Ngozumpa Glacier area and base DEM are from Thompson et al. (2016) displayed on a Landsat8 image (path/row: 140/41, acquired on 30 November 2014). Canwell Glacier data are from this study displayed on a Landsat7 image (path/row: 67/16, acquired on the 24 September 2010) draped over a 2010 DEM derived from airborne interferometric synthetic aperture radar (Geographic Information Network of Alaska, GINA; <http://ifsar.gina.alaska.edu/>).

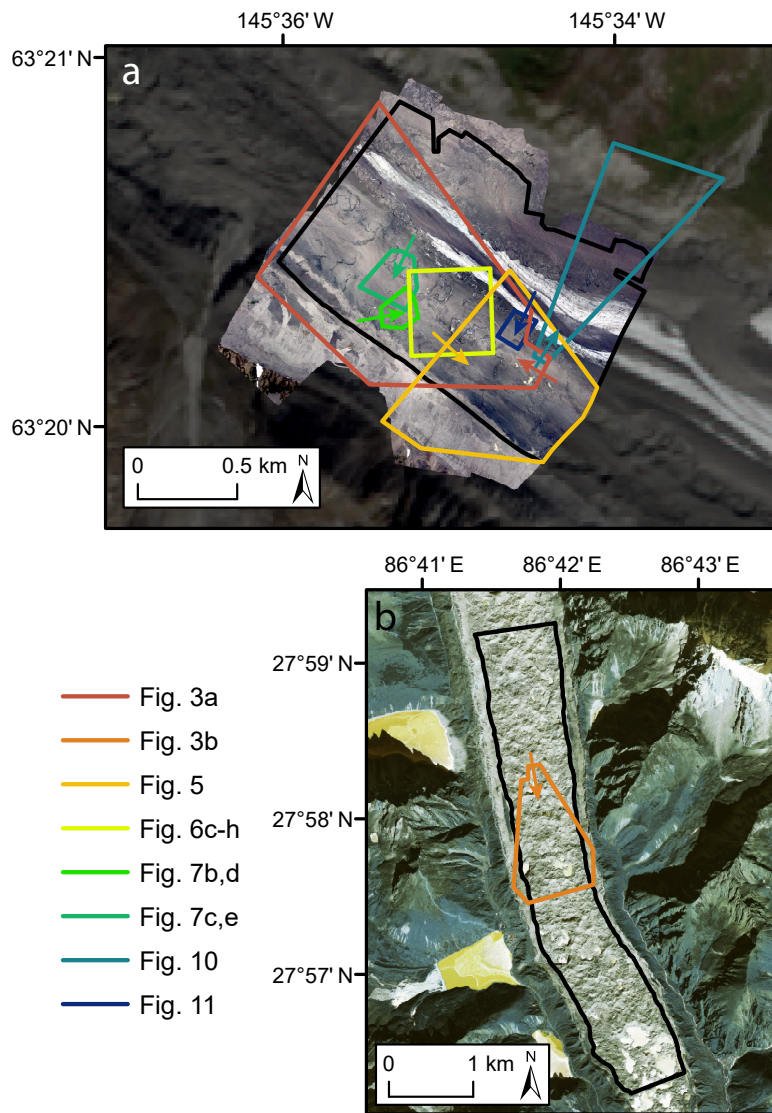


Figure 2. Study area location on Canwell Glacier (a) and Ngozumpa Glacier (b). The spatial domains over which the ice cliff mapping method was applied are shown in black. The location of subsequent map-based figures within this paper are shown. Arrows show the look direction of figures that have an oblique orientation. The base image shown in (a) is the orthomosaic collected on 29 July 1016 (Sect. 2.2.1) overlain on a Landsat8 image (path/row: 67/16) acquired on 31 August 2016; and (b) the GeoEye-1 image acquired on 23 December 2012 (Sect. 2.2.2).

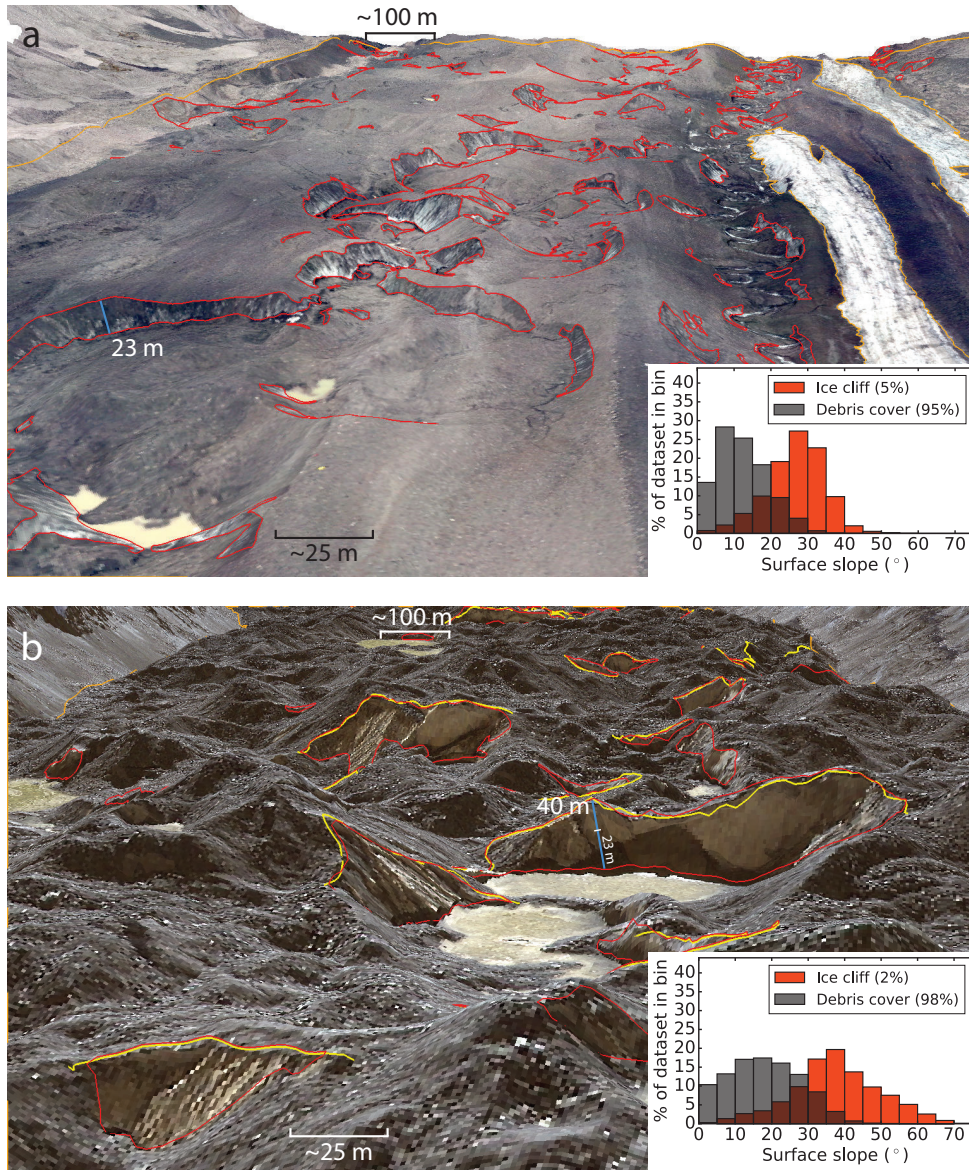


Figure 3. (a): portion of Canwell Glacier, Alaska, USA, looking down glacier, a distance of ~1.4 km. Manually generated debris-covered area outlines and ice cliffs (x) cliff outlines are outlined shown in orange and red, respectively. The inset histogram shows the normalized populations of surface slopes present in the pictured debris-covered and ice cliff area. The grey/orange region of overlap illustrates the difficulty of using surface slope alone to identify ice cliffs. Percentages give the fraction of the total area occupied by both classes (in map view). (b): same as panel (a) but for Ngozumpa Glacier, Nepal, also looking down glacier, a distance of ~1.4 km. The scale in panels (a) and (b) are the same. Yellow lines are ice cliff top edges mapped by Thompson et al. (2016) which were manually expanded to ice cliff area (red) with minor additions. Location shown in Fig. 2.

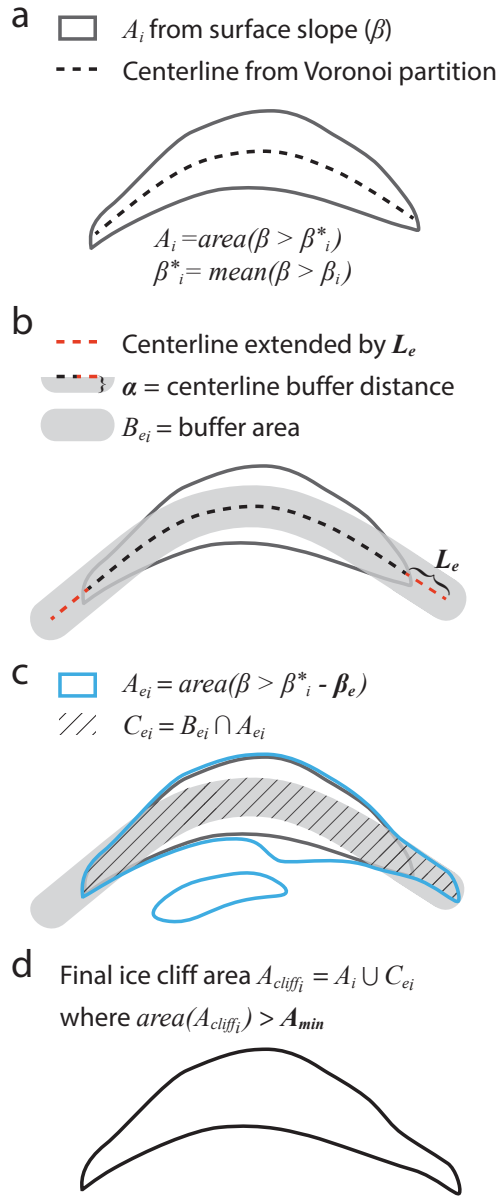


Figure 4. Method used to define ice cliff area, A_{cliff_i} for each iteration, i , and a final, optimized iteration, subscript opt . Surface slope threshold β_i is applied over the range 0-90° from which the subsequent quantities shown in steps a-d are calculated. Quantities in bold font are fixed scalar model parameters that do not vary over the iterative process. (a) shows how the area A_i is defined by β_{*i} , the mean surface slope of values constrained by β_i . A procedure using a Voronoi partition defines a centerline within A_i . (b) shows this centerline extended by a distance of L_e , and transformed into an area, B_{ei} , by an outward buffer distance, α , applied in all (x, y) directions. (c) shows the definition of A_{ei} , an area defined by a surface slope threshold lower than β_{*i} , where β_{*i} is reduced by β_e . The intersection of A_{ei} and the buffer area, B_{ei} , defines C_{ei} . C_{ei} allows the identification of ice cliff end area that has a surface slope below β_{*i} but above A_{ei} while rejecting area that falls within this same surface slope interval but is not located at the ends of an ice cliff. The intersection of A_i and C_{ei} , with areas below a threshold, A_{min} , removed defines the final ice cliff area, A_{cliff_i} , for that i (d).

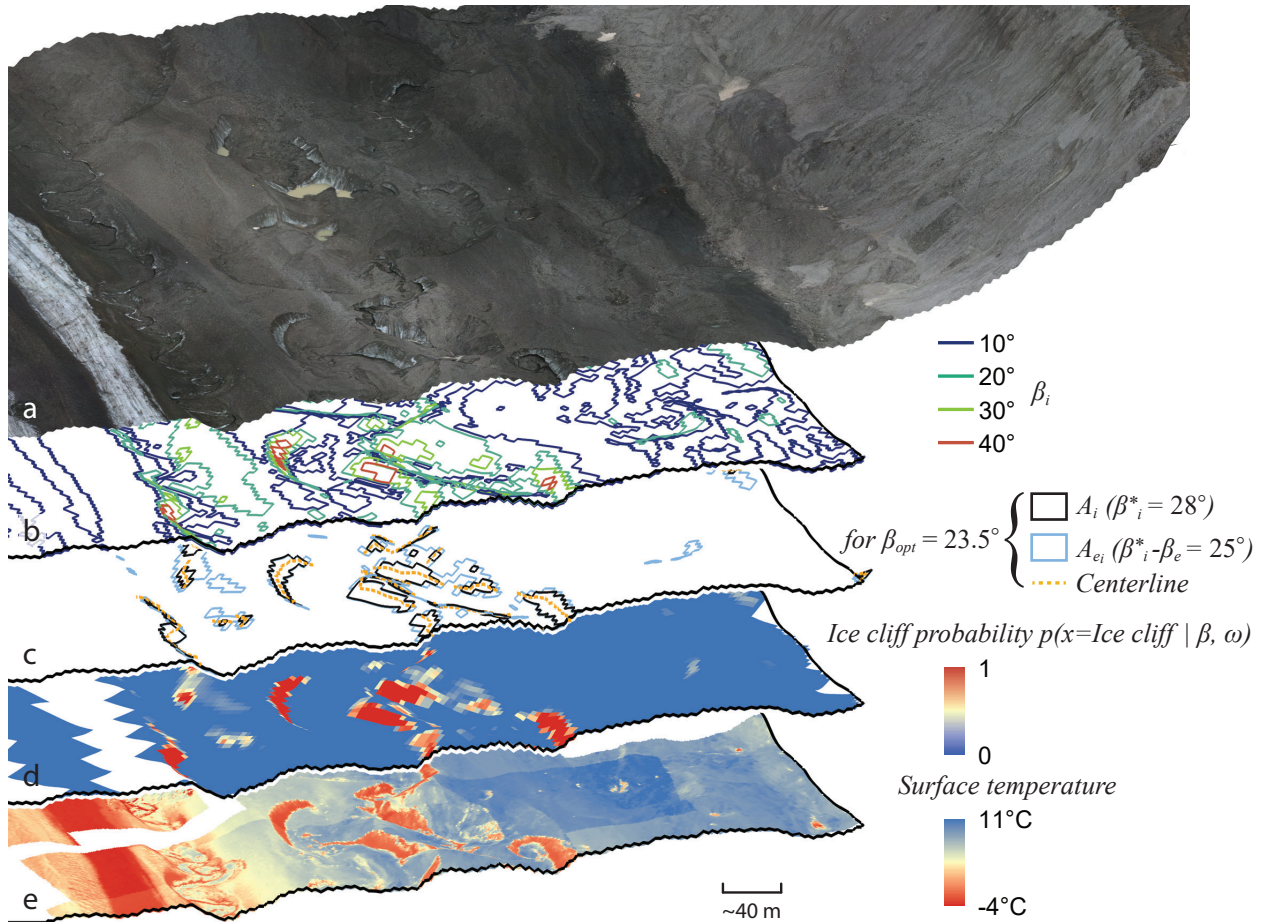


Figure 5. (a) orthomosaic of visible imagery collected above Canwell Glacier on 29 July 2016, draped over a DEM derived from the same images. (b) shows the area enclosed for select surface slope thresholds, β_i , during the iterative process. (c) shows intermediate quantities calculated during the final iteration using β_{opt} , the optimized β_i . The area enclosed by A_{e_i} and the ice cliff centerlines are used to add low angle area at the ends of ice cliffs to the area A_i , the main ice cliff shape defined from β_{i^*} . (d) shows the final distributed map of $p(x|\beta,\omega)p(x=Ice\ cliff|\beta,\omega)$, the computed probability that a given pixel will fall within true ice cliff area, x , assigned as a function of surface slope, β , and ω , the overlap with the final vector ice cliff shape, A_{cliff} , generated from the quantities shown in (c). (e) orthomosaic of thermal imagery collected on 29 July 2016, draped over the same DEM from (a). The color gradient is flipped so that cold ice cliffs easily stand out as red can be easily compared with (d). Location shown in Fig. 2.

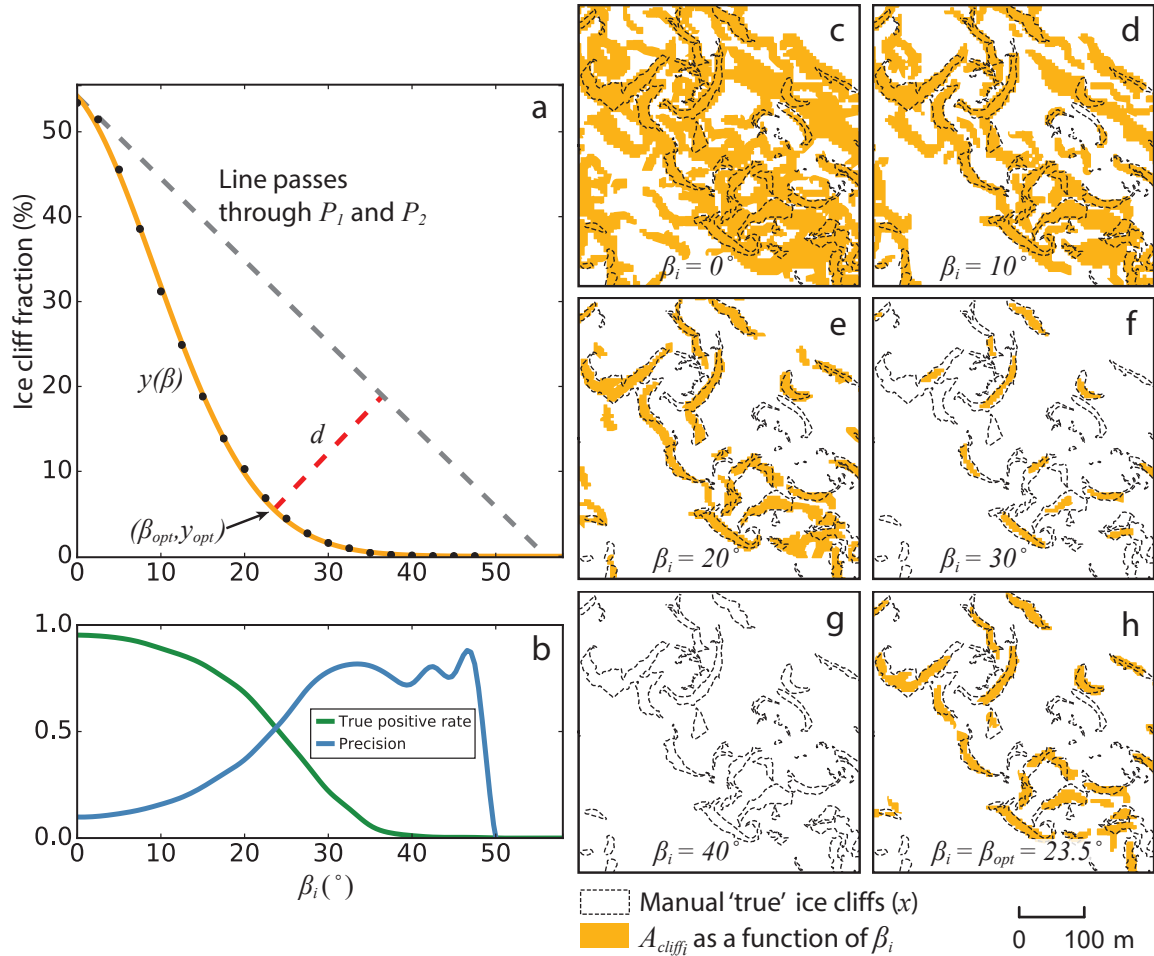


Figure 6. (a) shows the heuristic method for selecting β_{opt} . Black dots are computed values of the fraction of area ice cliffs occupy within the spatial domain for each β_i in n number of iterations (i). The orange curve, $y(\beta)$, is a **Gaussian** function fit to these points (Eq. (2)). β_{opt} is found by finding the longest distance, d , between $y(\beta)$ and a line passing through points P_1 and P_2 (Eq. (5) and Eq. (6)). β_{opt} is hypothesized to be coincident with the intersection of *true positive rate* and *precision*, the optimized, best possible balance of errors. (b) *true positive rate* and *precision* (derived in Sect. 3.5) comparing method results for each β_i to ‘true’ ice cliff area mapped from high resolution optical and thermal data (Sect. 2.2.1). (c-g) show the respective ice cliff maps (A_{cliff_i}) for x – axis ticks in (a) and (b) up to $\beta_i = 40^\circ$, with ‘true’ ice cliff area (x) overlain for reference. (h) shows the iterative method run a final time where $\beta_i = \beta_{opt}$ and defines the automatically selected best ice cliff map. Location of Panels c-h shown in Fig. 2.

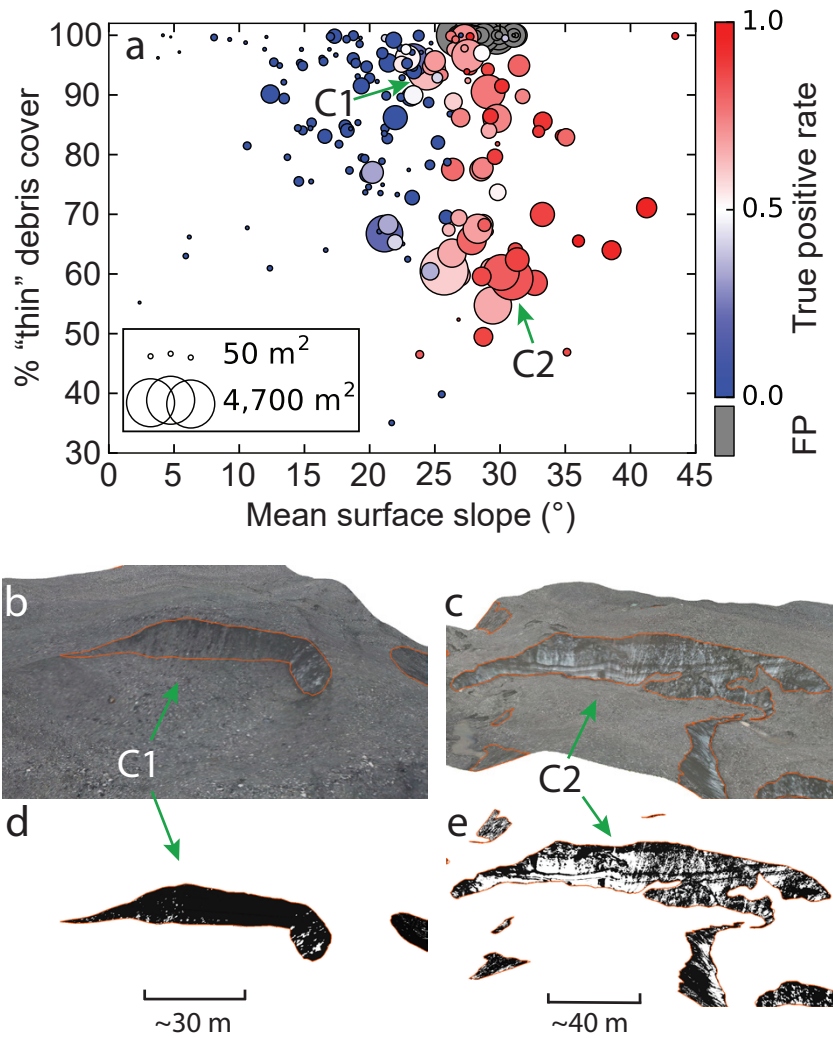


Figure 7. (a) each ‘true’ manually mapped ice cliff on the Canwell Glacier is shown as a circle sized proportionally to map view surface area and plotted against mean ice cliff surface slope and the percentage of “thin” debris cover on the ice cliff face. The color scale shows *true positive rate* from the automated ice cliff mapping method derived for each ice cliff. *FP* ice cliffs, defined as isolated shapes that are solely *FP* area and do not share a boundary with a ‘true’ ice cliff, are colored grey and abbreviated as *FP* on the axis label. Two ice cliffs (C1 and C2) are shown to illustrate how “thin” debris cover was mapped and provide context to the data presented in (a). (b) and (c) are oblique views of the 29 July 2016 Canwell Glacier orthomosaic with manually generated ice cliff outlines ~~from a~~ shown in orange. (d) and (e) are the same views with the orthomosaic processed to identify only debris cover on ice cliff faces. C1 is nearly 100% debris covered which could draw into question its classification as an ice cliff. C2 is one of the more “clean” ice cliffs within the Canwell Glacier study area but is still covered by a non-trivial amount, >50%, of debris. C1 shows linear englacial debris bands that contribute to the ice cliff face debris accumulation. Location shown in Fig. 2.

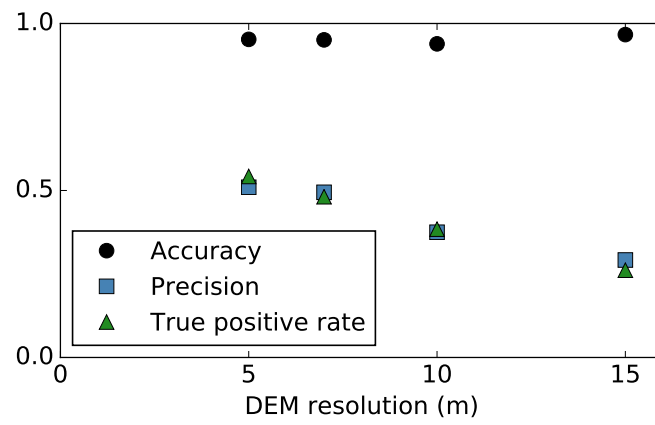


Figure 8. Method performance as a function of input DEM resolution.

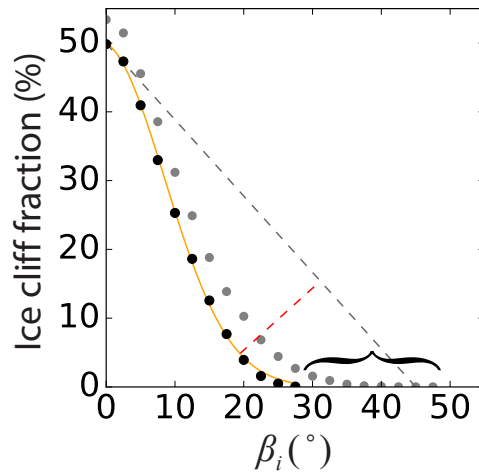


Figure 9. Identical to Fig. 6a, except with *TP* and *FP* area removed from the Canwell Glacier spatial domain to test the [tool+method](#) on an area that has definitively no ice cliffs. For comparison, dots shown in grey are the black dots in Fig. 6a where *TP* and *FP* area are not removed. The curly bracket shows the extension of the curve that is indicative of the presence of steep surface slope areas characteristic of ice cliffs. While the method still identified area (erroneously) as ice cliff, the abrupt termination of the curve with *TP* and *FP* area removed is an indication that there are in fact no ice cliffs present.

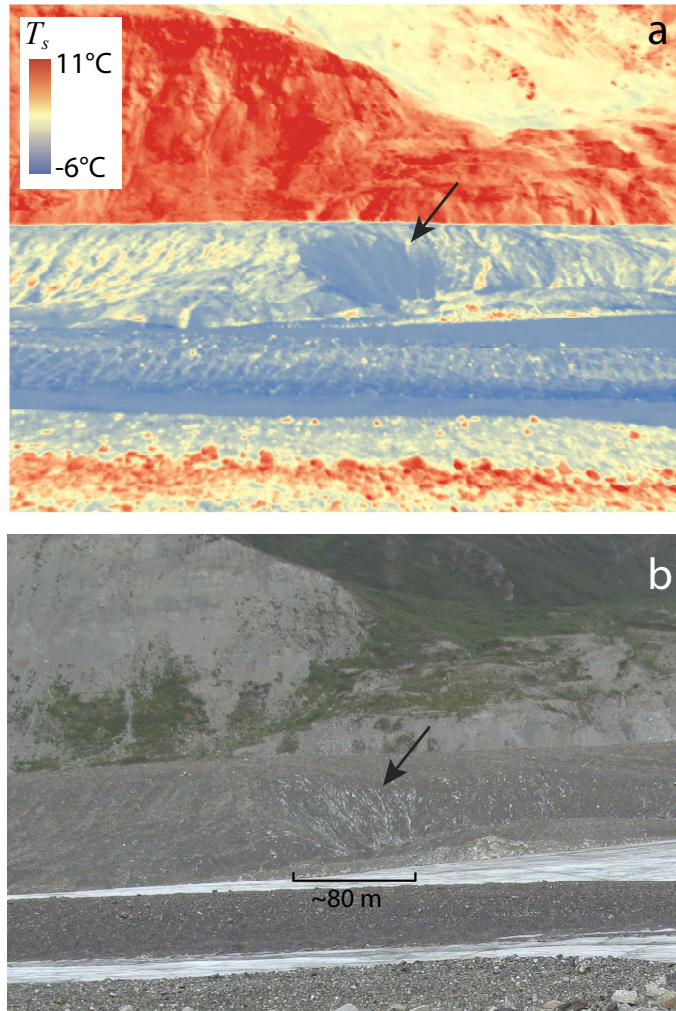


Figure 10. The side of a medial moraine on Canwell Glacier, possibly at an intermediate stage between being classified as an ice cliff or debris-covered area (black arrow in (a) and (b)). (a) oblique image of surface temperature (T_s). The sharp boundary between blue and red in the middle of the image separates the top of the medial moraine and the off-glacier valley wall. (b) oblique visible image of the same feature. Location shown in Fig. 2. Bare ice T_s values below 0°C are likely due to assuming a constant emissivity for the entire image.

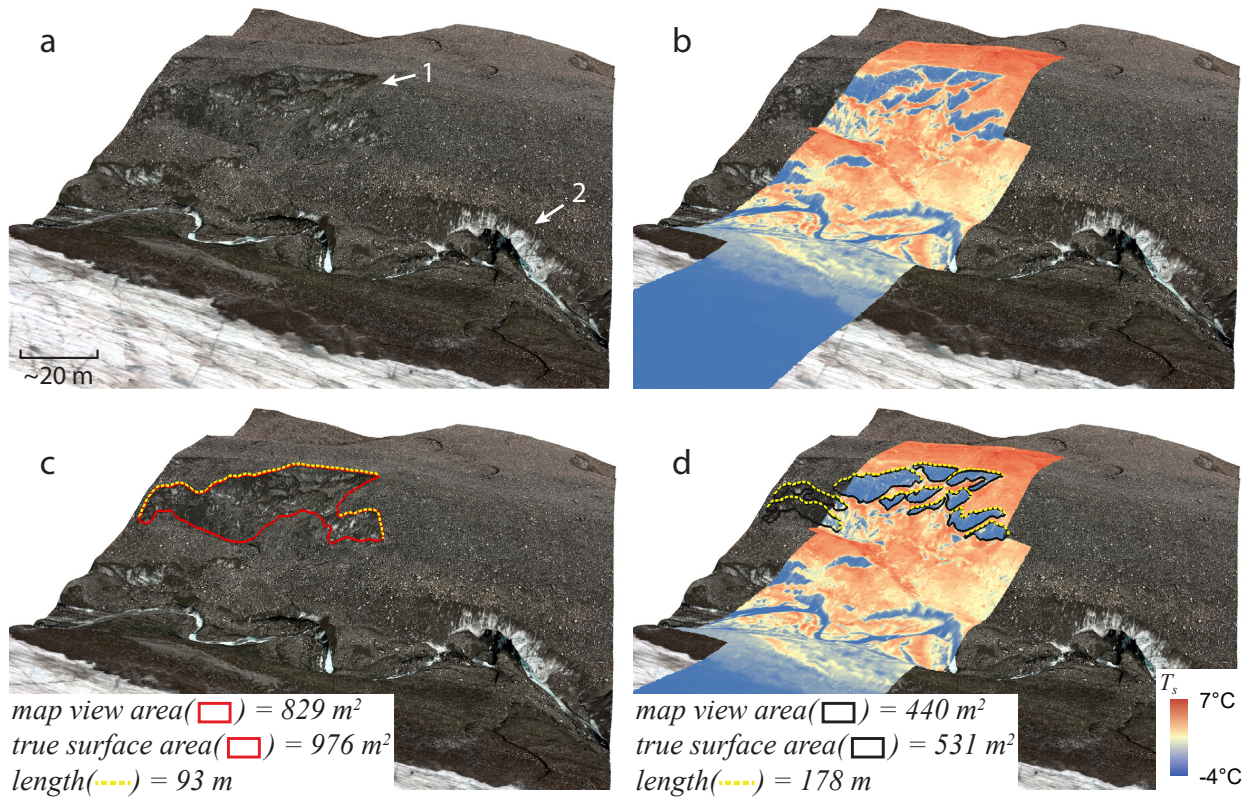


Figure 11. 1 and 2 in (a) show a less obvious and a very obvious ice cliff, respectively. When high resolution surface temperature (T_s) data is draped over ice cliff 1 in panel b, it becomes very apparent. (c) and (d) demonstrate two common methods for mapping ice cliffs: by area and by tracing the top edge. Bare ice T_s values below 0°C are likely due to assuming a constant emissivity for the entire image.